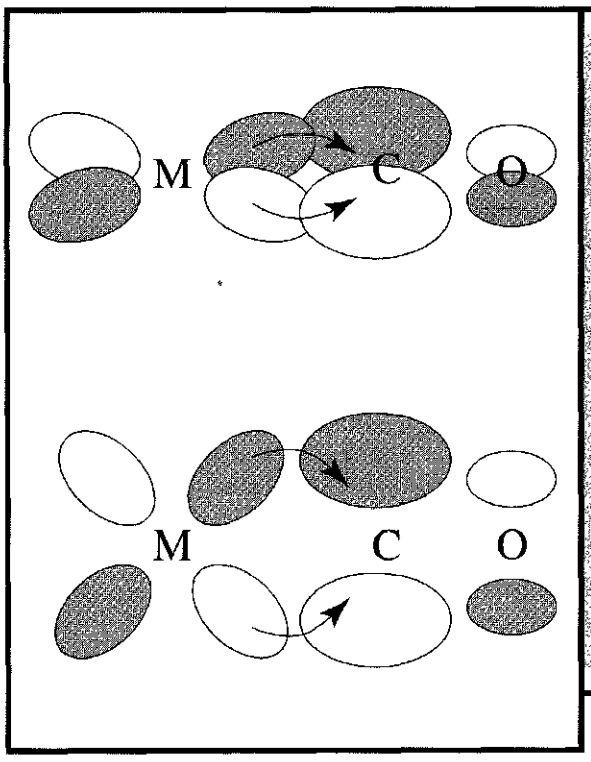

CHAPTER

10

Coordination Chemistry II: Bonding

10-1 EXPERIMENTAL EVIDENCE FOR ELECTRONIC STRUCTURES

Any theory of bonding in coordination complexes must explain the experimental behavior of the complexes. Some of the methods used most frequently to study these complexes are described here. These, and other methods, have been used to provide evidence for theories used to explain the electronic structure and bonding of coordination complexes.

10-1-1 THERMODYNAMIC DATA

One of the primary goals of a bonding theory must be to explain the energy of compounds. Experimentally, the energy is frequently not determined directly, but thermodynamic measurements of enthalpies and free energies of reaction are used to compare compounds.

Inorganic chemists, and coordination chemists in particular, frequently use **stability constants** (sometimes called **formation constants**) as indicators of bonding strengths (Table 10-1). These are the equilibrium constants for formation of coordination complexes, usually measured in aqueous solution. Examples of these reactions and corresponding stability constant expressions include the following:

$$[Fe(H_2O)_6]^{3+} + SCN^-(aq) \rightleftharpoons [FeSCN(H_2O)_5]^{2+} + H_2O \qquad K_1 = \frac{[FeSCN^{2+}]}{[Fe^{3+}][SCN^-]} = 9 \times 10^2$$

$$[Cu(H_2O)_6]^{2+} + 4\,NH_3(aq) \rightleftharpoons [Cu(NH_3)_4(H_2O)_2]^{2+} + 4\,H_2O \qquad K_4 = \frac{[Cu(NH_3)_4{}^{2+}]}{[Cu^{2+}][NH_3]^4} = 1 \times 10^{13}$$

(Water molecules have been omitted from the equilibrium constant expressions for simplicity.) The large stability constants indicate that bonding with the incoming ligand is much more favorable than bonding with water, although entropy effects must also be considered in equilibria.

heavier. With a paramagnetic sample, the tube and magnet attract each other and the magnet appears slightly lighter. The measurement of the known compound provides a standard from which the mass susceptibility (susceptibility per gram) of the sample can be calculated and converted to the molar susceptibility. More precise measurements require temperature control and measurement at different magnetic field strengths to correct for possible impurities.

Magnetic susceptibility (χ) is commonly measured in units of cm^3/mole; the **magnetic moment**, μ, is

$\mu = 2.828\ (\chi T)^{\frac{1}{2}}$ (T = Kelvin temperature) The unit of magnetic moment is the Bohr magneton, with 1 $\mu_B = 9.27 \times 10^{-24}$ J T^{-1} (joules/tesla).

Paramagnetism arises because electrons behave as tiny magnets. Although there is no direct evidence for spinning movement by electrons, a charged particle spinning rapidly would generate a **spin magnetic moment** and the popular term has therefore become **electron spin**. Electrons with $m_s = -\frac{1}{2}$ are said to have a negative spin; those with $m_s = +\frac{1}{2}$ have a positive spin. The total spin magnetic moment is characterized by the spin quantum number S, which is equal to the maximum total spin (sum of the m_s values). For example, an isolated oxygen atom with electron configuration $1s^2 2s^2 2p^4$ in its ground state has one electron in each of two $2p$ orbitals and a pair in the third. The total spin is $S = +\frac{1}{2} + \frac{1}{2} + \frac{1}{2} - \frac{1}{2} = 1$. The orbital angular momentum, characterized by the quantum number L, where L is equal to the maximum possible sum of the m_l values, results in an additional orbital magnetic moment. For the oxygen atom, the maximum possible sum of the m_l values for the p^4 electrons occurs when two electrons have $m_l = +1$ and one each have $m_l = 0$ and $m_l = -1$. In this case, $L = +1 + 0 - 1 + 1 = 1$. The combination of these two contributions to the magnetic moment, added as vectors, is the total magnetic moment of the atom or molecule. Additional details of quantum numbers S and L are provided in Chapter 11.

EXERCISE 10-1

Calculate L and S for the nitrogen atom.

The equation for the magnetic moment is

$$\mu_{S+L} = g\sqrt{[S(S+1)] + [\tfrac{1}{4}L(L+1)]}$$

where μ = magnetic moment
g = gyromagnetic ratio (conversion to magnetic moment)
S = spin quantum number
L = orbital quantum number

Although detailed determination of the electronic structure requires consideration of the orbital moment, for most complexes of the first transition series, the spin-only moment is sufficient, because any orbital contribution is small.

$$\mu_S = g\sqrt{S(S+1)}$$

External fields from other atoms and ions may effectively quench the orbital moment in these complexes. For the heavier transition metals and the lanthanides, the orbital contribution is larger and must be taken into account. Because we are usually concerned

primarily with the number of unpaired electrons in the compound, and the possible values of μ differ significantly for different numbers of unpaired electrons, the errors introduced by considering only the spin moment are usually not large enough to cause difficulty. From this point, we will consider only the spin moment.

In Bohr magnetons, the gyromagnetic ratio, g, is 2.00023, frequently rounded to 2. The equation for the **spin-only moment** μ_S, then becomes

$$\mu_S = 2\sqrt{S(S+1)} = \sqrt{4S(S+1)}$$

Because $S = \frac{1}{2}, 1, \frac{3}{2}, \ldots$ for $1, 2, 3, \ldots$, unpaired electrons, this equation can also be written

$$\mu_S = \sqrt{n(n+2)}$$

where n = number of unpaired electrons. This is the equation that is used most frequently. Table 10-3 shows the change in μ_S and μ_{S+L} with n, along with some experimental moments.

EXERCISE 10-2

Show that $\sqrt{4S(S+1)}$ and $\sqrt{n(n+2)}$ are equivalent expressions.

EXERCISE 10-3

Calculate the spin-only magnetic moment for the following atoms and ions. (Remember the order of loss of electrons from transition metals described near the end of Section 2-2-4.)

Fe $\quad Fe^{2+}$ $\quad$ Cr $\quad Cr^{3+}$ $\quad$ Cu $\quad Cu^{2+}$

There are several other techniques to measure magnetic susceptibility, including nuclear magnetic resonance[5] and the Faraday method using an unsymmetrical magnetic field.[6]

TABLE 10-3
Calculated and Experimental Magnetic Moments

Ion	n	S	L	μ_S	μ_{S+L}	*Observed*
V^{4+}	1	$\frac{1}{2}$	2	1.73	3.00	1.7–1.8
Cu^{2+}	1	$\frac{1}{2}$	2	1.73	3.00	1.7–2.2
V^{3+}	2	1	3	2.83	4.47	2.6–2.8
Ni^{2+}	2	1	3	2.83	4.47	2.8–4.0
Cr^{3+}	3	$\frac{3}{2}$	3	3.87	5.20	~3.8
Co^{2+}	3	$\frac{3}{2}$	3	3.87	5.20	4.1–5.2
Fe^{2+}	4	2	2	4.90	5.48	5.1–5.5
Co^{3+}	4	2	2	4.90	5.48	~5.4
Mn^{2+}	5	$\frac{5}{2}$	0	5.92	5.92	~5.9
Fe^{3+}	5	$\frac{5}{2}$	0	5.92	5.92	~5.9

SOURCE: F. A. Cotton and G. Wilkinson, *Advanced Inorganic Chemistry*, 4th ed., Wiley, New York, 1980, pp. 627–628.

NOTE: All moments are given in Bohr magnetons.

[5]D. F. Evans, *J. Chem. Soc.*, **1959**, 2003.

[6]L. N. Mulay and I. L. Mulay, *Anal. Chem.*, **1972**, *44*, 324R.

10-1-3 ELECTRONIC SPECTRA

Direct evidence of orbital energy levels can be obtained from electronic spectra. The energy of the light absorbed as electrons are raised to higher levels is the difference in energy between the states, which depend on the orbital energy levels and their occupancy. The observed spectra are frequently more complex than the simple energy diagrams used in this chapter seem to indicate; Chapter 11 gives a more complete picture of electronic spectra of coordination compounds. Much information about bonding and electronic structures in complexes has come from the study of electronic spectra.

10-1-4 COORDINATION NUMBERS AND MOLECULAR SHAPES

Although a number of factors influence the number of ligands bonded to a metal and the shapes of the resulting species, in some cases we can predict which structure is favored from the electronic structure of the complex. For example, two four-coordinate structures are possible, tetrahedral and square planar. Some metals, such as Pt(II), form almost exclusively square-planar complexes. Others, such as Ni(II) and Cu(II), exhibit both structures, depending on the ligands. Subtle differences in electronic structure, described later in this chapter, help to explain these differences.

10-2 THEORIES OF ELECTRONIC STRUCTURE

10-2-1 TERMINOLOGY

Different names have been used for the theoretical approaches to the electronic structure of coordination complexes, depending on the preferences of the authors. The labels we will use are described here, in order of their historical development:

Valence bond theory. This method describes bonding using hybrid orbitals and electron pairs, as an extension of the electron-dot and hybrid orbital methods used for simpler molecules. Although the theory as originally proposed is seldom used today, the hybrid notation is still common in discussing bonding.

Crystal field theory. This is an electrostatic approach, used to describe the split in metal *d*-orbital energies. It provides an approximate description of the electronic energy levels that determine the ultraviolet and visible spectra, but does not describe the bonding.

Ligand field theory. This is a more complete description of bonding in terms of the electronic energy levels of the frontier orbitals. It uses some of the terminology of crystal field theory but includes the bonding orbitals. However, most descriptions do not include the energy of these bonding orbitals.

Angular overlap method. This is a method of estimating the relative magnitudes of the orbital energies in a molecular orbital calculation. It explicitly takes into account the bonding energy as well as the relative orientation of the frontier orbitals.

In the following pages, the valence bond theory and the crystal field theory are described very briefly to set more recent developments in their historical context. The rest of the chapter describes the ligand field theory and the method of angular overlap, which can be used to estimate the orbital energy levels. These two supply the basic approach to bonding in coordination compounds for the remainder of the book.

10-2-2 HISTORICAL BACKGROUND

Valence bond theory

The valence bond theory, originally proposed by Pauling in the 1930s, uses the hybridization ideas presented in Chapter 5.[7] For octahedral complexes, d^2sp^3 hybrids of the metal orbitals are required. However, the d orbitals used by the first-row transition metals could be either $3d$ or $4d$. Pauling originally described the structures resulting from these as covalent and ionic, respectively. He later changed the terms to "hyperligated" and "hypoligated," and they are also known as inner orbital (using $3d$) and outer orbital (using $4d$) complexes. The number of unpaired electrons, measured by the magnetic behavior of the compounds, determines which d orbitals are used. Low spin and high spin are now used as more descriptive labels for the two configurations possible for d^4 through d^7 ions (discussed in Section 10-3-2).

Fe(III) has five unpaired electrons as an isolated ion, one in each of the $3d$ orbitals. In octahedral coordination compounds, it may have either one or five unpaired electrons. In complexes with one unpaired electron, the ligand electrons force the metal d electrons to pair up and leave two $3d$ orbitals available for hybridization and bonding. In complexes with five unpaired electrons, the ligands do not bond strongly enough to force pairing of the $3d$ electrons. Pauling proposed that the $4d$ orbitals could be used for bonding in such cases, with the arrangement of electrons shown in Figure 10-2.

When seven electrons must be provided for, as in Co(II), there are either one or three unpaired electrons. In the low-spin case with one unpaired electron, the seventh electron must go into a higher orbital (unspecified by Pauling, but presumed to be $5s$).[8] In the high-spin case with three unpaired electrons, the $4d$ or outer orbital hybrid must be used for bonding, leaving the metal electrons in the $3d$ levels. Similar arrangements are necessary for eight or nine electrons [Ni(II) and Cu(II)], although they frequently change geometry to either tetrahedral or square-planar structures.

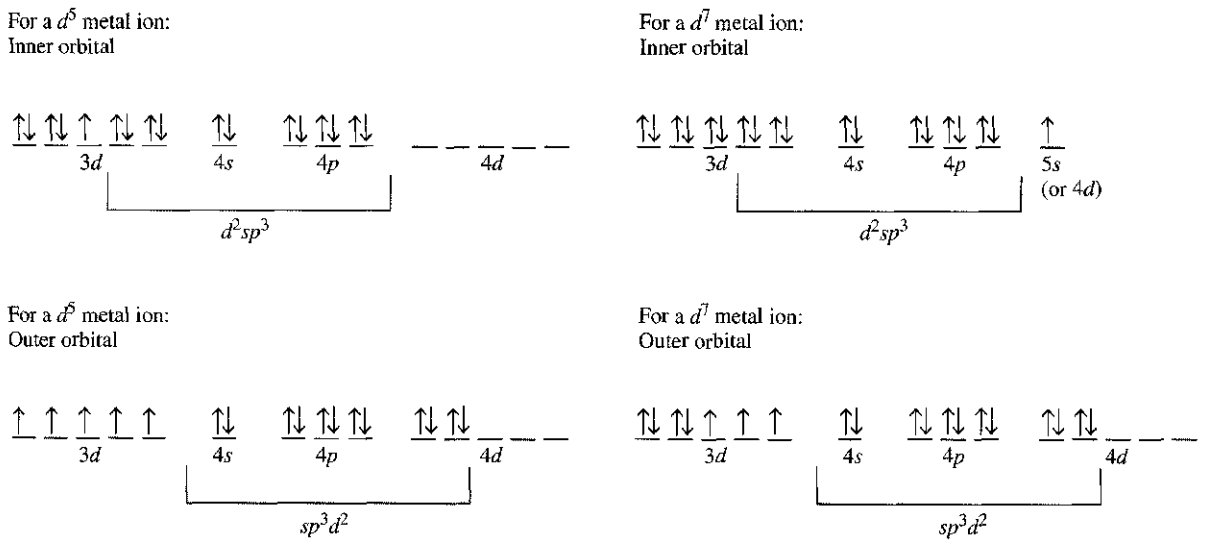

FIGURE 10-2 Inner and Outer Orbital Complexes. In each case, ligand electrons fill the d^2sp^3 bonding orbitals. The remaining orbitals contain the electrons from the metal.

[7] L. Pauling, *The Nature of the Chemical Bond*, 3rd ed., Cornell University Press, Ithaca, NY, 1960, Chapter 5.

[8] B. N. Figgis and R. S. Nyholm, *J. Chem. Soc.*, **1959**, 338; J. S. Griffith and L. E. Orgel, *Q. Rev. Chem. Soc.*, **1957**, XI, 381.

The valence bond theory was of great importance in the development of bonding theory for coordination compounds, but it is rarely used today except when discussing the hybrid orbitals used in bonding. Although it provided a set of orbitals for bonding, the use of the very high energy $4d$ orbitals seems unlikely, and the results do not lend themselves to a good explanation of the electronic spectra of complexes. Because much of our experimental data are derived from electronic spectra, this is a serious shortcoming.

Crystal field theory

As originally developed, crystal field theory[9] was used to describe the electronic structure of metal ions in crystals, where they are surrounded by oxide ions or other anions that create an electrostatic field with symmetry dependent on the crystal structure. The energies of the d orbitals of the metal ions are split by the electrostatic field, and approximate values for these energies can be calculated. No attempt was made to deal with covalent bonding, because the ionic crystals did not require it. Crystal field theory was developed in the 1930s. Shortly afterward, it was recognized that the same arrangement of charged or neutral electron pair donor species around a metal ion existed in crystals and in coordination complexes, and a more complete molecular orbital theory was developed.[10] However, neither was widely used until the 1950s, when interest in coordination chemistry increased.

When the d orbitals of a metal ion are placed in an octahedral field of ligand electron pairs, any electrons in them are repelled by the field. As a result, the $d_{x^2-y^2}$ and d_{z^2} orbitals, which are directed at the surrounding ligands, are raised in energy. The d_{xy}, d_{xz}, and d_{yz} orbitals, which are directed between the surrounding ions, are relatively unaffected by the field. The resulting energy difference is identified as Δ_o (o for octahedral; some older references use the term $10Dq$ instead of Δ_o). This approach provides a simple means of identifying the d-orbital splitting found in coordination complexes and can be extended to include more quantitative calculations. It requires extension to the more complete ligand field theory to include π bonding and more accurate calculations of the resulting energy levels.

The average energy of the five d orbitals is above that of the free ion orbitals, because the electrostatic field of the ligands raises their energy. The t_{2g} orbitals are $0.4\Delta_o$ below and the e_g orbitals are $0.6\Delta_o$ above this average energy, as shown in Figure 10-3. The three t_{2g} orbitals then have a total energy of $-0.4\Delta_o \times 3 = -1.2\Delta_o$ and the two e_g orbitals have a total energy of $+0.6\Delta_o \times 2 = +1.2\Delta_o$ compared with the average.

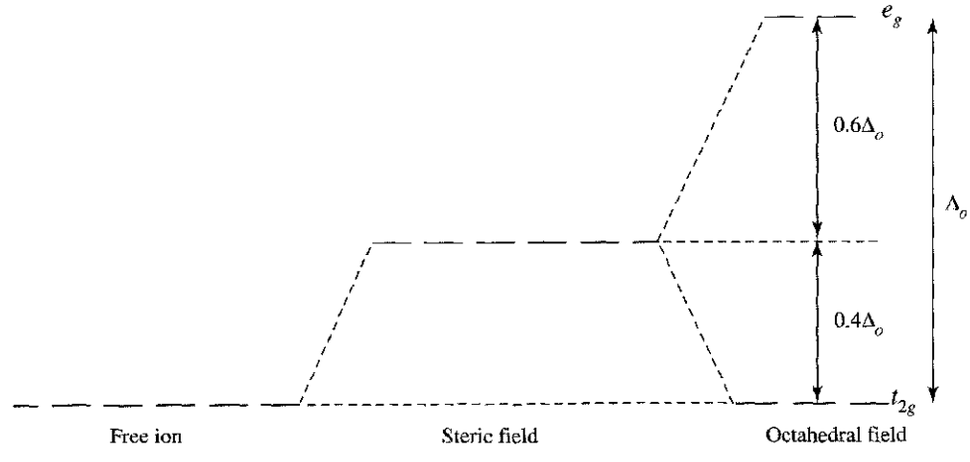

FIGURE 10-3 Crystal Field Splitting.

[9] H. Bethe, *Ann. Phys.*, **1929**, *3*, 133.
[10] J. H. Van Vleck, *J. Chem. Phys.*, **1935**, *3*, 807.

The energy difference between the actual distribution of electrons and that for all electrons in the uniform field levels is called the **crystal field stabilization energy** (CFSE). It is equal in magnitude to the ligand field stabilization energy (LFSE) described later in this chapter.

The chief drawbacks to the crystal field approach are in its concept of the repulsion of orbitals by the ligands and its lack of any explanation for bonding in coordination complexes. As we have seen in all our discussions of molecular orbitals, any interaction between orbitals leads to both higher and lower energy molecular orbitals. The purely electrostatic approach does not allow for the lower (bonding) molecular orbitals, and thus fails to provide a complete picture of the electronic structure.

10-3 LIGAND FIELD THEORY

The electrostatic crystal field theory and the molecular orbital theory were combined into a more complete theory called ligand field theory, described qualitatively by Griffith and Orgel.[11] Many of the details presented here come from their work.

10-3-1 MOLECULAR ORBITALS FOR OCTAHEDRAL COMPLEXES

For octahedral complexes, the molecular orbitals can be described as resulting from a combination of a central metal atom accepting a pair of electrons from each of six σ donor ligands. The interaction of these ligands with some of the metal d orbitals is shown in Figure 10-4. The $d_{x^2-y^2}$ and d_{z^2} orbitals can form bonding orbitals with the ligand orbitals, but the d_{xy}, d_{xz}, and d_{yz} orbitals cannot form bonding orbitals. Bonding interactions are possible with the s (weak, but uniformly with all the ligands) and the p orbitals of the metal, with one pair of ligand orbitals interacting with each p orbital.

The six ligand donor orbitals collectively form a reducible representation Γ in the point group O_h. This representation can be reduced by the method described in Section 4-4-2 applied to the character table in Table 10-4. This results in $\Gamma = A_{1g} + T_{1u} + E_g$, shown in the last rows of the table.

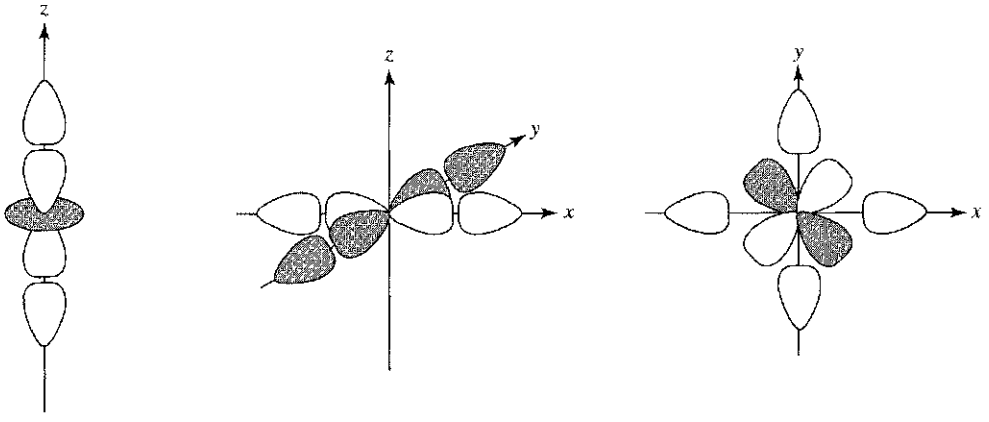

Bonding interaction between two ligand orbitals and metal d_{z^2} orbital

Bonding interaction between four ligand orbitals and metal $d_{x^2-y^2}$ orbital

Nonbonding (no interaction) four ligand orbitals and metal d_{xy} orbital

FIGURE 10-4 Orbital Interactions in Octahedral Complexes.

[11] J. S. Griffith and L. E. Orgel, *Q. Rev. Chem. Soc.*, **1957**, XI, 381.

TABLE 10-4
Character table for O_h

O_h	E	$8C_3$	$6C_2$	$6C_4$	$3C_2(=C_4^2)$	i	$6S_4$	$8S_6$	$3\sigma_h$	$6\sigma_d$		
A_{1g}	1	1	1	1	1	1	1	1	1	1		
A_{2g}	1	1	−1	−1	1	1	−1	1	1	−1		
E_g	2	−1	0	0	2	2	0	−1	2	0		$(2z^2 - x^2 - y^2, x^2 - y^2)$
T_{1g}	3	0	−1	1	−1	3	1	0	−1	−1	(R_x, R_y, R_z)	
T_{2g}	3	0	1	−1	−1	3	−1	0	−1	1		(xy, xz, yz)
A_{1u}	1	1	1	1	1	−1	−1	−1	−1	−1		
A_{2u}	1	1	−1	−1	1	−1	1	−1	−1	1		
E_u	2	−1	0	0	2	−2	0	1	−2	0		
T_{1u}	3	0	−1	1	−1	−3	−1	0	1	1	(x, y, z)	
T_{2u}	3	0	1	−1	−1	−3	1	0	1	−1		
Γ	6	0	0	2	2	0	0	0	4	2		$x^2 + y^2 + z^2$
A_{1g}	1	1	1	1	1	1	1	1	1	1		
T_{1u}	3	0	−1	1	−1	−3	−1	0	1	1	(x, y, z)	
E_g	2	−1	0	0	2	2	0	−1	2	0		$(2z^2 - x^2 - y^2, x^2 - y^2)$

The six ligand σ_{donor} orbitals (p orbitals or hybrid orbitals with the same symmetry) match the symmetries of the $4s$, $4p_x$, $4p_y$, $4p_z$, $3d_{z^2}$, and $3d_{x^2-y^2}$ metal orbitals. The combination of the ligand and metal orbitals form six bonding and six antibonding orbitals with a_{1g}, e_g, and t_{1u} symmetries. The six bonding orbitals are filled by electrons donated by the ligands. The metal T_{2g} orbitals (d_{xy}, d_{xz}, and d_{yz}) do not have appropriate symmetry to interact with the ligands and are nonbonding. Any electrons of the metal occupy these orbitals and the higher energy antibonding orbitals.

The set of σ energy levels common to all octahedral complexes is shown in Figure 10-5. All π interactions are ignored for the moment. They will be discussed later in Section 10-3-3.

Most of the discussion of octahedral ligand fields is concentrated on the t_{2g} and higher orbitals. Electrons in bonding orbitals provide the potential energy that holds molecules together. Electrons in the higher levels affected by ligand field effects help determine the details of the structure, magnetic properties, and electronic spectrum.

10-3-2 ORBITAL SPLITTING AND ELECTRON SPIN

In octahedral coordination complexes, electrons from the ligands fill all six bonding molecular orbitals, and any electrons from the metal ion occupy the nonbonding t_{2g} and the antibonding e_g orbitals. The split between these two sets of orbitals (t_{2g} and e_g) is called Δ_o (o for octahedral). Ligands whose orbitals interact strongly with the metal orbitals are called **strong-field ligands**. With these, the split between the t_{2g} and e_g orbitals is large, and as a result Δ_o is large. Ligands with small interactions are called **weak-field ligands**; the split between the t_{2g} and e_g orbitals is smaller and Δ_o is small. For d^0 through d^3 and d^8 through d^{10} ions, only one electron configuration is possible,

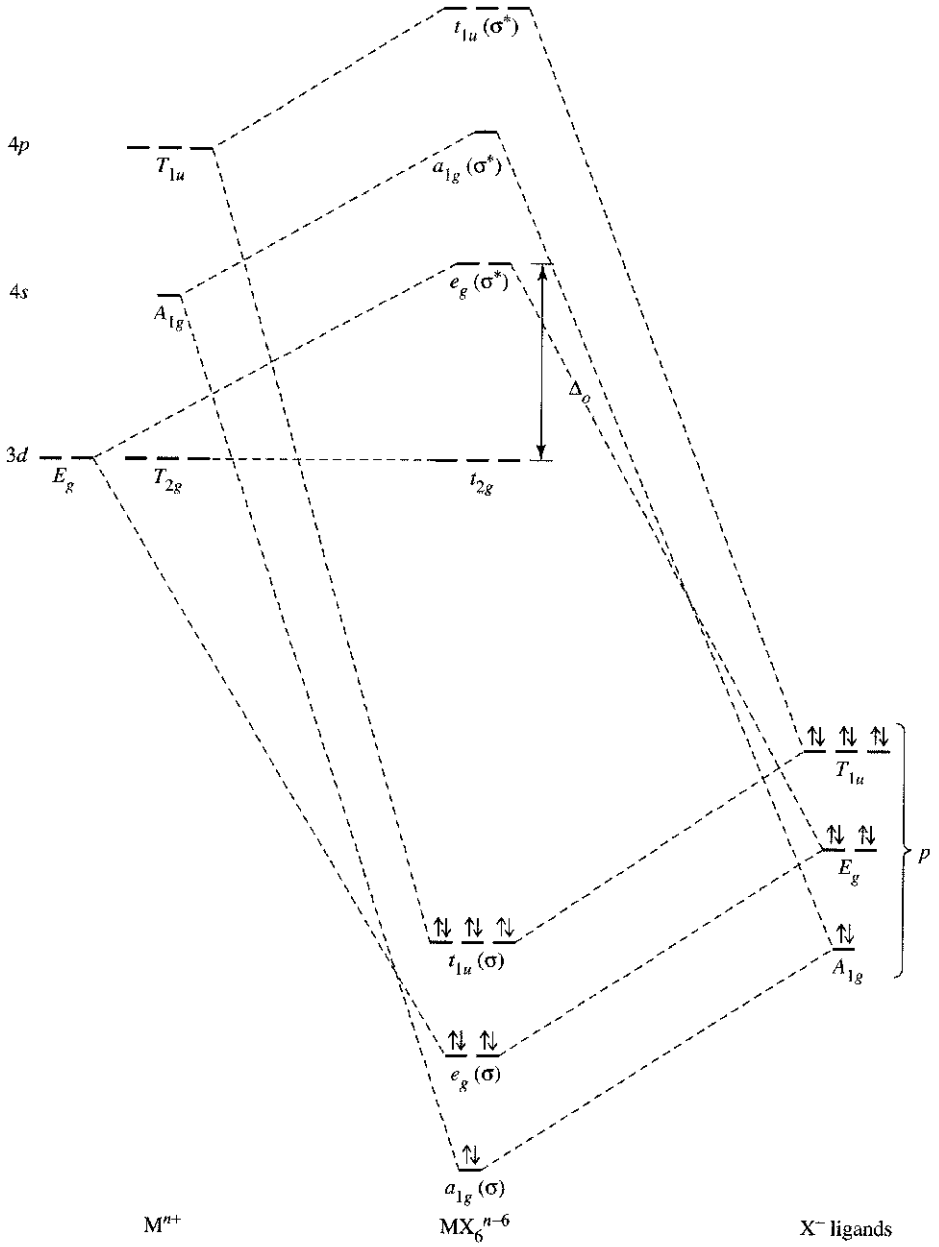

FIGURE 10-5 Molecular Orbitals for an Octahedral Transition Metal Complex. As in Chapter 5, the symmetry labels of the atomic orbitals are capitalized and the labels of the molecular orbitals are in lowercase. (Adapted from F. A. Cotton, *Chemical Applications of Group Theory*, 3rd ed., Wiley-Interscience, New York, 1990, p. 232, omitting π orbitals. © 1990, John Wiley & Sons, Inc. Reprinted by permission of John Wiley & Sons, Inc.)

so there is no difference in the net spin of the electrons for strong- and weak-field cases. On the other hand, the d^4 through d^7 ions exhibit **high-spin** and **low-spin** states, as shown in Table 10-5. Strong ligand fields lead to low-spin complexes, and weak ligand fields lead to high-spin complexes.

Terminology for these configurations is summarized as follows:

$$\text{Strong ligand field} = \text{large } \Delta_o = \text{low spin}$$

$$\text{Weak ligand field} = \text{small } \Delta_o = \text{high spin}$$

As explained in Section 2-2-3, the energy of pairing two electrons depends on the Coulombic energy of repulsion between two electrons in the same region of space, Π_c, and the purely quantum mechanical exchange energy, Π_e. The relationship between the

TABLE 10-5
Spin States and Ligand Field Strength

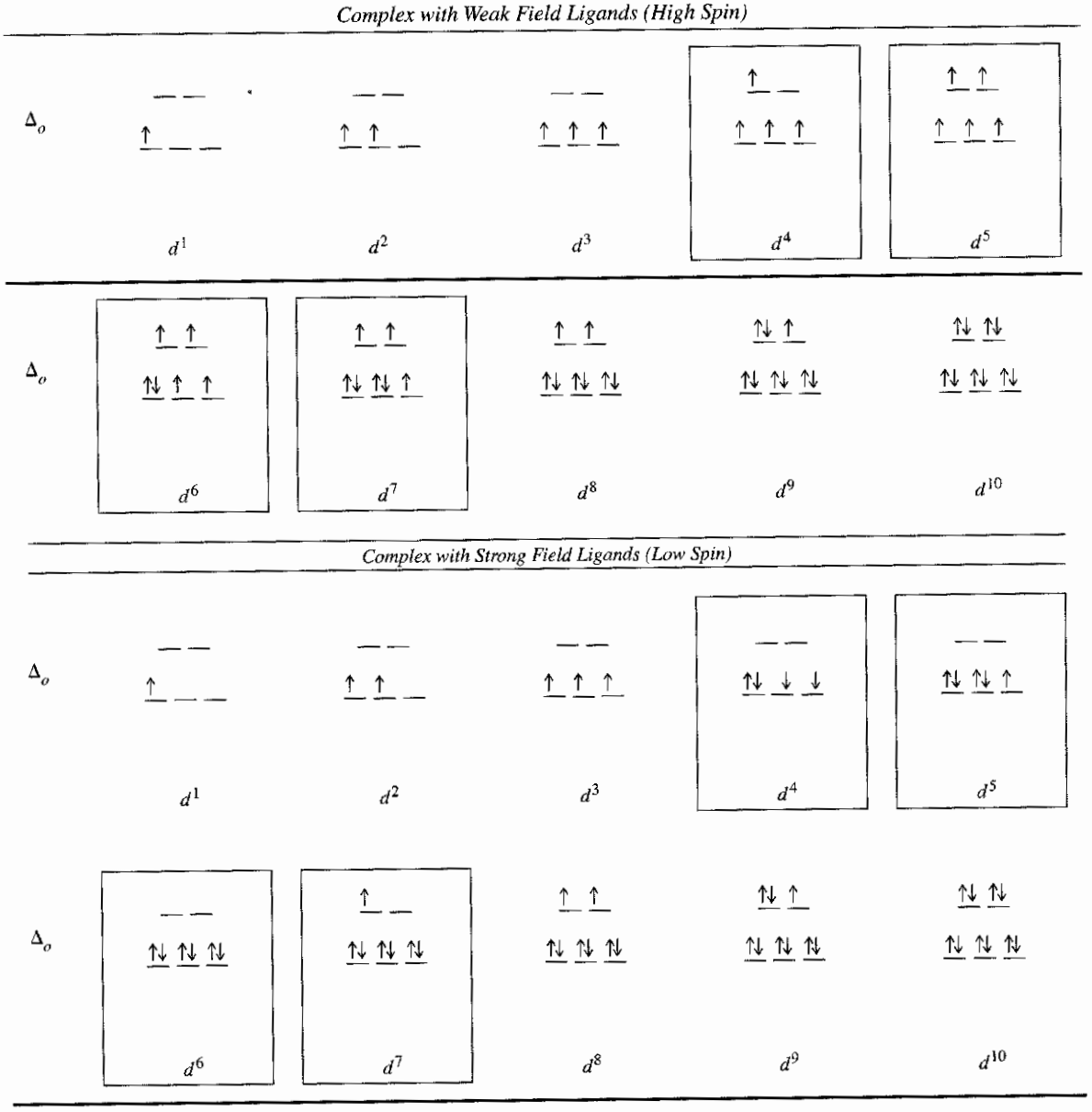

difference between the t_{2g} and e_g energy levels, the Coulombic energy, and the exchange energy (Δ_o, Π_c, and Π_e respectively) determines the orbital configuration of the electrons. The configuration with the lower total energy is the ground state for the complex. Remember that Π_c is a *positive* energy, indicating less stability, and Π_e is a *negative* energy, indicating more stability.

For example, a d^5 ion could have five unpaired electrons, three in t_{2g} and two in e_g orbitals, as a **high-spin** case or it could have only one unpaired electron, with all five electrons in the t_{2g} levels, as a **low-spin** case. The possibilities for all cases, d^1 through d^{10}, are given in Table 10-5.

EXAMPLE

Determine the exchange energies for high-spin and low-spin d^6 ions in an octahedral complex.

A d^6 ion has four exchangeable pairs in a high-spin complex and six in a low-spin complex.

In the high-spin complex, the electron spins are as shown on the right. The five ↑ electrons have exchangeable pairs 1-2, 1-3, 2-3, and 4-5, for a total of four. The exchange energy is therefore $4\Pi_e$. Only electrons at the same energy can exchange.

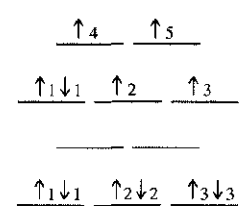

In the low-spin complex, as shown on the right, each set of three electrons with the same spin has exchangeable pairs 1-2, 1-3, and 2-3, for a total of six, and the exchange energy is $6\Pi_e$.

The difference between the high-spin and low-spin complexes is two exchangeable pairs.

EXERCISE 10-4

Find the exchange energy for a d^5 ion, both as a high-spin and as a low-spin complex.

The change in exchange energy from high spin to low spin is zero for d^5 ions and favorable (negative) for d^6 ions. The pairing energy is the same (two new pairs formed), as shown in Table 10-5. Overall, the change is energetically easier for d^6 ions.

Unlike the total pairing energy Π, Δ_o is strongly dependent on the ligands and on the metal. Table 10-6 presents values of Δ_o for aqueous ions, in which water is a relatively weak-field ligand (small Δ_o). In general, Δ_o for 3+ ions is larger than Δ_o for 2+ ions with the same number of electrons, and values for d^5 ions are smaller than for d^4 and d^6 ions. The number of unpaired electrons in the complex depends on the balance between Δ_o and Π. When $\Delta_o > \Pi$, there is a net loss in energy (increase in stability) on pairing electrons in the lower levels and the low-spin configuration is more stable; when $\Delta_o < \Pi$, the total energy is lower with more unpaired electrons and the high-spin configuration is more stable. In Table 10-6, only Co^{3+} has Δ_o near the size of Π, and $[Co(H_2O)_6]^{3+}$ is the only low-spin aqua complex. All the other first-row transition metal ions require a stronger field ligand than water for a low-spin configuration.

TABLE 10-6
Orbital Splitting (Δ_o) and Mean Pairing Energy (Π) for Aqueous Ions[a]

	Ion	Δ_o	Π	*Ion*	Δ_o	Π
d^1				Ti^{3+}	18,800	
d^2				V^{3+}	18,400	
d^3	V^{2+}	12,300		Cr^{3+}	17,400	
d^4	Cr^{2+}	9,250	23,500	Mn^{3+}	15,800	28,000
d^5	Mn^{2+}	7,850[b]	25,500	Fe^{3+}	14,000	30,000
d^6	Fe^{2+}	9,350	17,600	Co^{3+}	16,750	21,000
d^7	Co^{2+}	8,400	22,500	Ni^{3+}		27,000
d^8	Ni^{2+}	8,600				
d^9	Cu^{2+}	7,850				
d^{10}	Zn^{2+}	0				

SOURCES: For Δ_o: M^{2+} data from D. A. Johnson and P. G. Nelson, *Inorg. Chem.*, **1995**, *34*, 5666; M^{3+} data from D. A. Johnson and P. G. Nelson, *Inorg. Chem.*, **1999**, *38*, 4949. For Π: Data from D. S. McClure, The Effects of Inner-orbitals on Thermodynamic Properties, in T. M. Dunn, D. S. McClure, and R. G. Pearson, *Some Aspects of Crystal Field Theory*, Harper & Row, New York, 1965, p. 82.

NOTE: [a] Values given are in cm^{-1}.

[b] Estimated value.

Another factor that influences electron configurations and the resulting spin is the position of the metal in the periodic table. Metals from the second and third transition series form low-spin complexes more readily than metals from the first transition series. This is a consequence of two cooperating effects: one is the greater overlap between the larger $4d$ and $5d$ orbitals and the ligand orbitals, and the other is a decreased pairing energy due to the larger volume available for electrons in the $4d$ and $5d$ orbitals as compared with $3d$ orbitals.

10-3-3 LIGAND FIELD STABILIZATION ENERGY

The difference between (1) the total energy of a coordination complex with the electron configuration resulting from ligand field splitting of the orbitals and (2) the total energy for the same complex with all the d orbitals equally populated is called the **ligand field stabilization energy**, or **LFSE**. The LFSE represents the stabilization of the d electrons because of the metal-ligand environment. A common way to calculate LFSE is shown in Figure 10-6. The interaction of the d orbitals of the metal with the orbitals of the ligands results in a lower energy for the t_{2g} set of orbitals ($-\frac{2}{5}\Delta_o$ relative to the average energy of all t_{2g} and e_g orbitals) and an increased energy for the e_g set ($\frac{3}{5}\Delta_o$). The total energy of a one-electron system would then be $-\frac{2}{5}\Delta_o$ and the total energy of a high-spin four-electron system would be $\frac{3}{5}\Delta_o + 3(-\frac{2}{5}\Delta_o) = -\frac{3}{5}\Delta_o$. An alternative method of arriving at these energies is given by Cotton.[12]

EXERCISE 10-5

Find the LFSE for a d^6 ion for both high-spin and low-spin cases.

Table 10-7 has the LFSE values for σ-bonded octahedral complexes with one through ten electrons in both high- and low-spin arrangements. These values are commonly used as approximations even when significant π bonding is included. The final columns in Table 10-7 show the difference in LFSE between low-spin and high-spin complexes with the same total number of d electrons and the associated pairing energies. For one to three and eight to ten electrons, there is no difference in the number of unpaired electrons or the LFSE. For four to seven electrons, there is a significant difference in both.

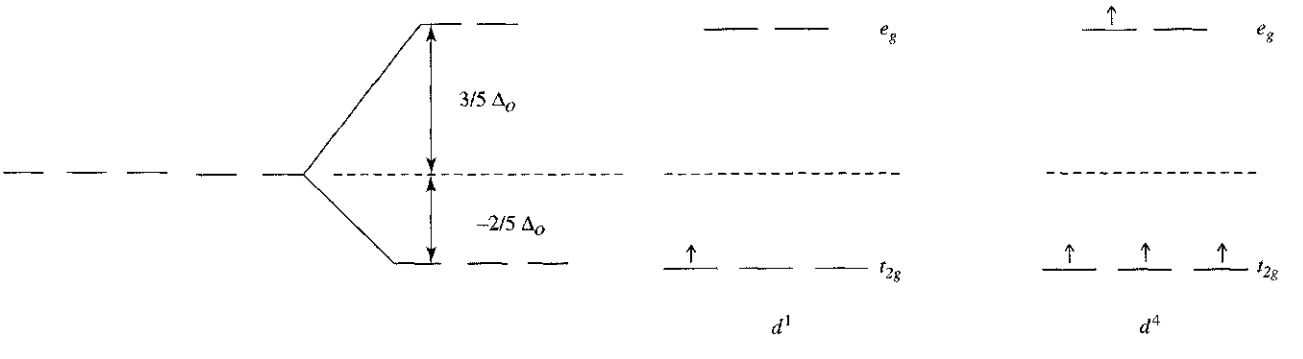

FIGURE 10-6 Splitting of Orbital Energies in a Ligand Field.

[12]F. A. Cotton, *J. Chem. Educ.*, **1964**, *41*, 466.

TABLE 10-7
Ligand Field Stabilization Energies

Number of d Electrons	*Weak-Field Arrangement* t_{2g}			e_g		*LFSE* (Δ_o)	*Coulombic Energy*	*Exchange Energy*
1	↑					$-\frac{2}{5}$		
2	↑	↑				$-\frac{4}{5}$		Π_e
3	↑	↑	↑			$-\frac{6}{5}$		$3\Pi_e$
4	↑	↑	↑	↑		$-\frac{3}{5}$		$3\Pi_e$
5	↑	↑	↑	↑	↑	0		$4\Pi_e$
6	↑↓	↑	↑	↑	↑	$-\frac{2}{5}$	Π_c	$4\Pi_e$
7	↑↓	↑↓	↑	↑	↑	$-\frac{4}{5}$	$2\Pi_c$	$5\Pi_e$
8	↑↓	↑↓	↑↓	↑	↑	$-\frac{6}{5}$	$3\Pi_c$	$7\Pi_e$
9	↑↓	↑↓	↑↓	↑↓	↑	$-\frac{3}{5}$	$4\Pi_c$	$7\Pi_e$
10	↑↓	↑↓	↑↓	↑↓	↑↓	0	$5\Pi_c$	$8\Pi_e$

Number of d Electrons	*Strong-Field Arrangement* t_{2g}			e_g		*LFSE* (Δ_o)	*Coulombic Energy*	*Exchange Energy*	*Strong Field − Weak Field*
1	↑					$-\frac{2}{5}$			0
2	↑	↑				$-\frac{4}{5}$		Π_e	0
3	↑	↑	↑			$-\frac{6}{5}$		$3\Pi_e$	0
4	↑↓	↑	↑			$-\frac{8}{5}$	Π_c	$3\Pi_e$	$-\Delta_o + \Pi_c$
5	↑↓	↑↓	↑			$-\frac{10}{5}$	$2\Pi_c$	$4\Pi_e$	$-2\Delta_o + 2\Pi_c$
6	↑↓	↑↓	↑↓			$-\frac{12}{5}$	$3\Pi_c$	$6\Pi_e$	$-2\Delta_o + 2\Pi_c + 2\Pi_e$
7	↑↓	↑↓	↑↓	↑		$-\frac{9}{5}$	$3\Pi_c$	$6\Pi_e$	$-\Delta_o + \Pi_c + \Pi_e$
8	↑↓	↑↓	↑↓	↑	↑	$-\frac{6}{5}$	$3\Pi_c$	$7\Pi_e$	0
9	↑↓	↑↓	↑↓	↑↓	↑	$-\frac{3}{5}$	$4\Pi_c$	$7\Pi_e$	0
10	↑↓	↑↓	↑↓	↑↓	↑↓	0	$5\Pi_c$	$8\Pi_e$	0

NOTE: In addition to the LFSE, each pair formed has a positive Coulombic energy, Π_c, and each set of two electrons with the same spin has a negative exchange energy, Π_e. When $\Delta_o > \Pi_c$ for d^4 or d^5 or when $\Delta_o > \Pi_c + \Pi_e$ for d^6 or d^7, the strong-field arrangement (low spin) is favored.

The most common example of LFSE in thermodynamic data appears in the exothermic enthalpy of hydration of bivalent ions of the first transition series, usually assumed to have six waters of hydration:

$$M^{2+}(g) + 6\,H_2O(l) \longrightarrow [M(H_2O)_6]^{2+}(aq)$$

Ions with spherical symmetry should have ΔH becoming increasingly exothermic (more negative) continuously across the transition series due to the decreasing radius of the ions with increasing nuclear charge and corresponding increase in electrostatic attraction for the ligands. Instead, the enthalpies show the characteristic double-loop shape shown in Figure 10-7, where ΔH is plotted. The almost linear curve of the "corrected" enthalpies is expected for ions with decreasing radius. The differences between this curve and the double-humped experimental values are approximately equal to the LFSE values in Table 10-7 for high-spin complexes,[13] with additional

[13]L. E. Orgel, *J. Chem. Soc.*, **1952**, 4756; P. George and D. S. McClure, *Prog. Inorg. Chem.*, **1959**, *1*, 381.

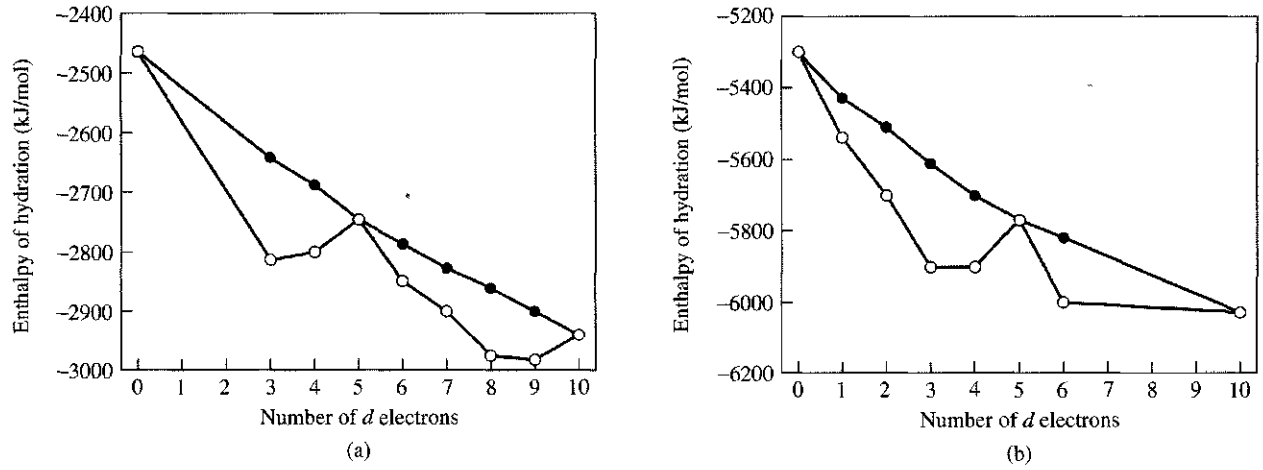

o Experimental values
• Corrected values

FIGURE 10-7 Enthalpies of Hydration of Transition Metal Ions. The lower curves show experimental values; the upper curves result when contributions from spin-orbit splitting, a relaxation effect from contraction of the metal-ligand distance, and interelectronic repulsion energy are subtracted. (a) 2+ ions. (b) 3+ ions. (Reproduced with permission from D. A. Johnson and P. G. Nelson, *Inorg. Chem.*, **1995**, *34*, 5666 (M^{2+} data); and D. A. Johnson and P. G. Nelson, *Inorg. Chem.*, **1999**, 4949 (M^{3+} data). © *1995, 1999*, American Chemical Society.)

smaller corrections for spin-orbit splittings (0 to 16 kJ/mol), a relaxation effect caused by contraction of the metal-ligand distance (0 to 24 kJ/mol), and an interelectronic repulsion energy that depends on the exchange interactions between electrons with the same spins (0 to −19 kJ/mol for M^{2+}, 0 to −156 kJ/mol for M^{3+}).[14] The net effect of the latter three effects is small, but improves the shape of the parabolic curve for the corrected values significantly. In the case of the hexaaqua and hexafluoro complexes of the 3+ transition metal ions, the interelectronic repulsion energy (sometimes called the nephelauxetic effect) is larger, and is required to remove the deviation from a smooth curve through the d^0, d^5, and d^{10} values.

Why do we care about LFSE? There are two principal reasons. First, it provides a more quantitative approach to the high-spin–low-spin electron configurations, helping predict which configuration will be more likely. Second, it is the basis for our later discussion of the spectra of these complexes. Measurements of Δ_o are commonly provided in studies of these complexes, with a goal of eventually allowing a better and more quantitative understanding of the bonding interactions. At this point, the relative sizes of Δ_o, Π_c, and Π_e are the important features.

10-3-4 PI BONDING

The description of LFSE and bonding in coordination complexes given up to this point has included only σ-donor ligands. Addition of the other ligand orbitals allows the possibility of π bonding. This addition involves the other p or π^* orbitals of the ligands (those that are not involved in σ bonding). The axes for the ligand atoms can be chosen

[14] D. A. Johnson and P. G. Nelson, *Inorg. Chem.*, **1995**, *34*, 3253; **1995**, *34*, 5666; **1999**, *38*, 4949.

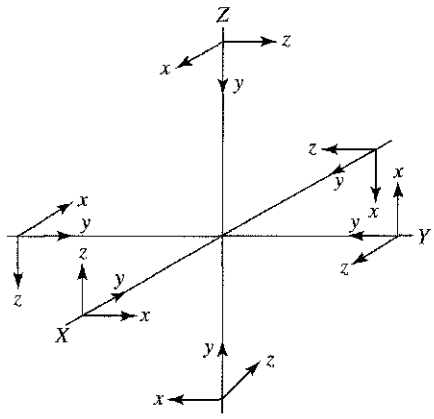

FIGURE 10-8 Coordinate System for Octahedral π Orbitals.

in any consistent way. In Figure 10-8, the y axes are pointing toward the metal atom. The x and z axes (which are appropriate for π symmetry) make a right-handed set at each ligand, with the directions chosen to avoid a bias in any direction. Opposite ligands have x axes at right angles to each other, and z axes are also perpendicular.

The x and z axes (and their corresponding orbitals) must be taken as a single set of 12, because each axis can be converted into every other axis by one of the symmetry operations (C_4 or one of the σ). The reducible representation for these 12 orbitals is in the top row of Table 10-8. The reducible representation is

$$\Gamma_\pi = T_{1g} + T_{2g} + T_{1u} + T_{2u}$$

EXERCISE 10-6

Show that the representations in Table 10-8 can be obtained from the orbitals in Figure 10-8.

Of these four representations, T_{1g} and T_{2u} have no match among the metal orbitals, T_{2g} matches the d_{xy}, d_{xz}, d_{yz} orbitals, and T_{1u} matches the p_x, p_y, p_z orbitals of the metal. The p orbitals of the metal are already used in σ bonding and will not overlap well with the ligand π orbitals because of the larger bond distances in coordination complexes; therefore, they are unlikely to be used also for π bonding. There are then three orbitals on the metal (d_{xy}, d_{xz}, d_{yz}) available for π bonds distributed over the six ligand-metal pairs. The t_{2g} orbitals of the metal, which are nonbonding in the σ-only orbital calculations shown in Figure 10-5, participate in the π interaction to produce a lower bonding set and a higher antibonding set.

Pi bonding in coordination complexes is possible when the ligand has p or π^* molecular orbitals available. Because the effects are smaller for occupied orbitals, we will first treat the more important case of ligands with empty π^* orbitals, or π-acceptor ligands.

TABLE 10-8
Representations of Octahedral π Orbitals

O_h	E	$8C_3$	$6C_2$	$6C_4$	$3C_2(=C_4^2)$	i	$6S_4$	$8S_6$	$3\sigma_h$	$6\sigma_d$	
Γ_π	12	0	0	0	−4	0	0	0	0	0	
T_{1g}	3	0	−1	1	−1	3	1	0	−1	−1	
T_{2g}	3	0	1	−1	−1	3	−1	0	−1	1	(d_{xy}, d_{xz}, d_{yz})
T_{1u}	3	0	−1	1	−1	−3	−1	0	1	1	(p_x, p_y, p_z)
T_{2u}	3	0	1	−1	−1	−3	1	0	1	−1	

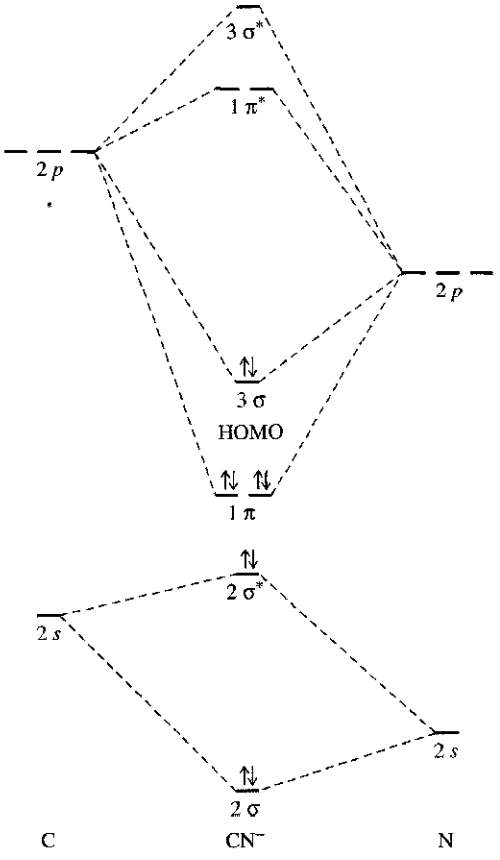

FIGURE 10-9 Cyanide Molecular Orbitals.

The cyanide ion (Figure 10-9) provides an example. The molecular orbital picture of CN^- is intermediate between those of N_2 and CO given in Chapter 5, because the energy differences between C and N orbitals are significant but less than those between C and O orbitals. The HOMO for CN^- is a σ orbital with considerable bonding character and a concentration of electron density on the carbon. This is the donor orbital used by CN^- in forming σ orbitals in the complex. Above the HOMO, the LUMO orbitals of CN^- are two empty π^* orbitals that can be used for π bonding with the metal. Overlap of ligand orbitals with metal *d* orbitals is shown in Figure 10-10.

The ligand π^* orbitals have energies slightly higher than those of the metal t_{2g} (d_{xy}, d_{xz}, d_{yz}) orbitals, with which they overlap. As a result, they form molecular orbitals, with the bonding orbitals lower in energy than the initial metal t_{2g} orbitals. The corresponding antibonding orbitals are higher in energy than the e_g σ antibonding orbitals. Metal ion *d* electrons occupy the bonding orbitals (now the HOMO), resulting in a larger value for Δ_o and increased bonding strength, as shown in Figure 10-11(a). Significant energy stabilization can result from this added π bonding. This **metal-to-**

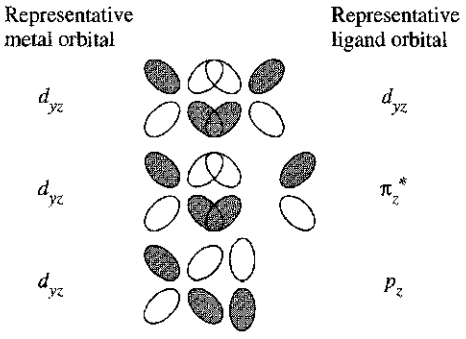

FIGURE 10-10 Overlap of *d*, π^*, and *p* Orbitals with Metal *d* Orbitals. Overlap is good with ligand *d* and π^* orbitals, but poorer with ligand *p* orbitals.

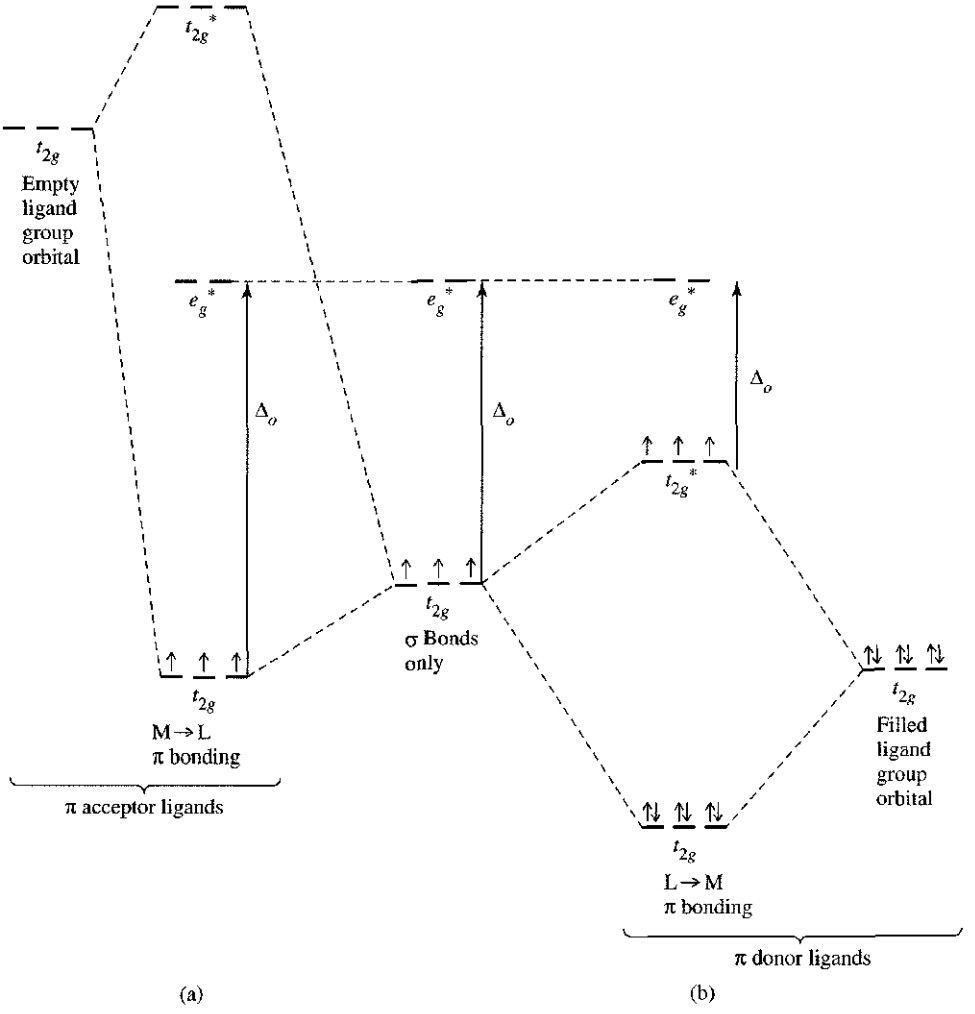

FIGURE 10-11 Effects of π Bonding on Δ_o (using a d^3 ion as example).

ligand (M ⟶ L) π bonding is also called **π back-bonding**, with electrons from *d* orbitals of the metal donated back to the ligands.

When the ligand has electrons in its *p* orbitals (as in F^- or Cl^-), the bonding molecular π orbitals will be occupied by these electrons, and there are two net results: the t_{2g} bonding orbitals (derived primarily from ligand orbitals) strengthen the ligand-metal linkage slightly, and the corresponding t_{2g}^* levels (derived primarily from metal *d* orbitals) are raised in energy and become antibonding. This reduces Δ_o, as in Figure 10-11(b). The metal ion *d* electrons are pushed into the higher t_{2g}^* orbital by the ligand electrons. This is described as **ligand-to-metal (L ⟶ M) π bonding**, with the π electrons from the ligands being donated to the metal ion. Ligands participating in such interactions are called π-donor ligands. The decrease in the energy of the bonding orbitals is partly counterbalanced by the increase in the energy of the t_{2g}^* orbitals. In addition, the combined σ and π donations from the ligands give the metal more negative charge, which decreases attraction between the metal and the ligands and makes this type of bonding less favorable.

Overall, filled π* or *p* orbitals on ligands (frequently with relatively low energy) result in L ⟶ M π bonding and a smaller Δ_o for the overall complex. Empty higher energy π or *d* orbitals on the ligands result in M ⟶ L π bonding and a larger Δ_o for the complex. Ligand-to-metal π bonding usually gives decreased stability for the complex, favoring high-spin configurations; metal-to-ligand π bonding usually gives increased stability and favors low-spin configurations.

Part of the stabilizing effect of π back-bonding is a result of transfer of negative charge away from the metal ion. The positive ion accepts electrons from the ligands to form the σ bonds. The metal is then left with a large negative charge. When the π orbitals can be used to transfer part of this charge back to the ligands, the overall stability is improved. The π-acceptor ligands that can participate in π back-bonding are extremely important in organometallic chemistry and will be discussed further in Chapter 13.

· Complexes with π bonding will have LFSE values modified by the changes in the t_{2g} levels described previously. Many good π-acceptor ligands form complexes with large differences between t_{2g} and e_g levels. The changes in energy levels caused by these different effects can be calculated by the angular overlap method covered in Section 10-4.

10-3-5 SQUARE-PLANAR COMPLEXES

Sigma bonding

The same general approach works for any geometry, although some are more complicated than others. Square-planar complexes such as $[Ni(CN)_4]^{2-}$, with D_{4h} symmetry, provide an example. As before, the axes for the ligand atoms are chosen for convenience. The y axis of each ligand is directed toward the central atom, the x axis is in the plane of the molecule, and the z axis is perpendicular to the plane of the molecule, as shown in Figure 10-12. The p_y set of ligand orbitals is used in σ bonding. Unlike the octahedral case, there are two distinctly different sets of potential π-bonding orbitals, the parallel set ($\pi_\parallel$ or p_x, in the molecular plane) and the perpendicular set ($\pi_\perp$ or p_z, perpendicular to the plane). By taking each set in turn, we can use the techniques of Chapter 4 to find the representations that fit the different symmetries. Table 10-9 gives the results.

The matching metal orbitals for σ bonding in the first transition series are those with lobes in the x and y directions, $3d_{x^2-y^2}$, $4p_x$, and $4p_y$, with some contribution from the less directed $3d_{z^2}$ and $4s$. Ignoring the other orbitals for the moment, we can construct the energy level diagram for the σ bonds, as in Figure 10-13. Comparing Figures 10-5 and 10-13, we see that the square-planar diagram looks more complex because the lower symmetry results in sets with less degeneracy than in the octahedral case. D_{4h} symmetry splits the d orbitals into three single representations (a_{1g}, b_{1g}, and b_{2g}, for d_{z^2}, $d_{x^2-y^2}$, and d_{xy} respectively) and the degenerate e_g for the d_{xz}, d_{yz} pair. The b_{2g} and e_g levels are nonbonding (no ligand σ orbital matches their symmetry) and the difference between them and the antibonding a_{1g} level corresponds to Δ.

EXERCISE 10-7

Derive the reducible representations for square-planar bonding and then show that their component irreducible representations are those in Table 10-9.

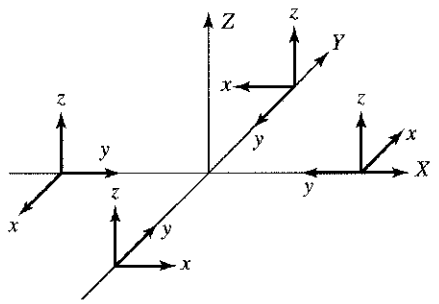

FIGURE 10-12 Coordinate System for Square-Planar Orbitals.

TABLE 10-9
Representations and Orbital Symmetry for Square-Planar Complexes

D_{4h}	E	$2C_4$	C_2	$2C_2'$	$2C_2''$	i	$2S_4$	σ_h	$2\sigma_v$	$2\sigma_d$		
A_{1g}	1	1	1	1		1	1	1	1	1		$x^2 + y^2, z^2$
A_{2g}	1	1	1	−1		1	1	1	−1	−1	R_z	
B_{1g}	1	−1	1	1		1	−1	1	1	−1		$x^2 - y^2$
B_{2g}	1	−1	1	−1		1	−1	1	−1	1		xy
E_g	2	0	−2	0		2	0	−2	0	0	(R_x, R_y)	(xz, yz)
A_{1u}	1	1	1	1		−1	−1	−1	−1	−1		
A_{2u}	1	1	1	−1		−1	−1	−1	1	1	z	
B_{1u}	1	−1	1	1		−1	1	−1	−1	1		
B_{2u}	1	1	1	−1		−1	1	−1	1	−1		
E_u	2	0	−2	0		−2	0	2	0	0	(x, y)	

D_{4h}	E	$2C_4$	C_2	$2C_2'$	$2C_2''$	i	$2S_4$	σ_h	$2\sigma_v$	$2\sigma_d$	
Γ_{p_x}	4	0	0	−2		0	0	4	−2	0	$p_\parallel$
Γ_{p_y}	4	0	0	2		0	0	4	2	0	p_σ
Γ_{p_z}	4	0	0	−2		0	0	−4	2	0	$p_\perp$

$\Gamma_{p_y} = A_{1g} + B_{1g} + E_u$ (σ) Matching orbitals on the central atom: $s, d_{z^2}, d_{x^2-y^2}, (p_x, p_y)$

$\Gamma_{p_x} = A_{2g} + B_{2g} + E_u$ ($\parallel$) Matching orbitals on the central atom: $d_{xy}, (p_x, p_y)$

$\Gamma_{p_z} = A_{2u} + B_{2u} + E_g$ ($\perp$) Matching orbitals on the central atom: $p_z, (d_{xz}, d_{yz})$

Pi bonding

The π-bonding orbitals are also shown in Table 10-9. The d_{xy} (b_{2g}) orbital interacts with the p_x $(\pi_\parallel)$ ligand orbitals, and the d_{xz} and d_{yz} (e_g) orbitals interact with the p_z $(\pi_\perp)$ ligand orbitals, as shown in Figure 10-14. The b_{2g} orbital is in the plane of the molecule. The two e_g orbitals have lobes above and below the plane. The p_y and p_z orbitals of the metal have the proper symmetry to form π bonds, but do not usually overlap effectively with the ligand orbitals. The results of these interactions are shown in Figure 10-15, as calculated for $[Pt(CN)_4]^{2-}$.

This diagram shows all the orbitals and is very complex. At first, it may seem overwhelming, but it can be understood if taken bit by bit. The π and π^* ligand orbitals are labeled parallel (for those in the plane of the complex, in the x direction) and perpendicular (for those perpendicular to the plane of the complex, in the z direction). The molecular orbitals are more easily described in the groups set off by boxes in the figure. The lowest energy set contains the bonding orbitals, as in the simpler σ-bonding diagram. Eight electrons from the ligand orbitals fill them. The next higher set consists of the eight π-donor orbitals of the ligand, essentially lone pairs on a simple halide ion or π orbitals on CN^-. Their interaction with the metal orbitals is small and has the effect of decreasing the energy difference between the orbitals of the next higher set. The third set of molecular orbitals is primarily metal d orbitals, modified by interaction with the ligand orbitals. The order of these orbitals has been described in several ways, depending on the detailed method used in the calculations.[15] The order shown is that found by

[15]T. Ziegler, J. K. Nagle, J. G. Snijders, and E. J. Baerends, *J. Am. Chem. Soc.*, **1989**, *111*, 5631, and the references cited therein.

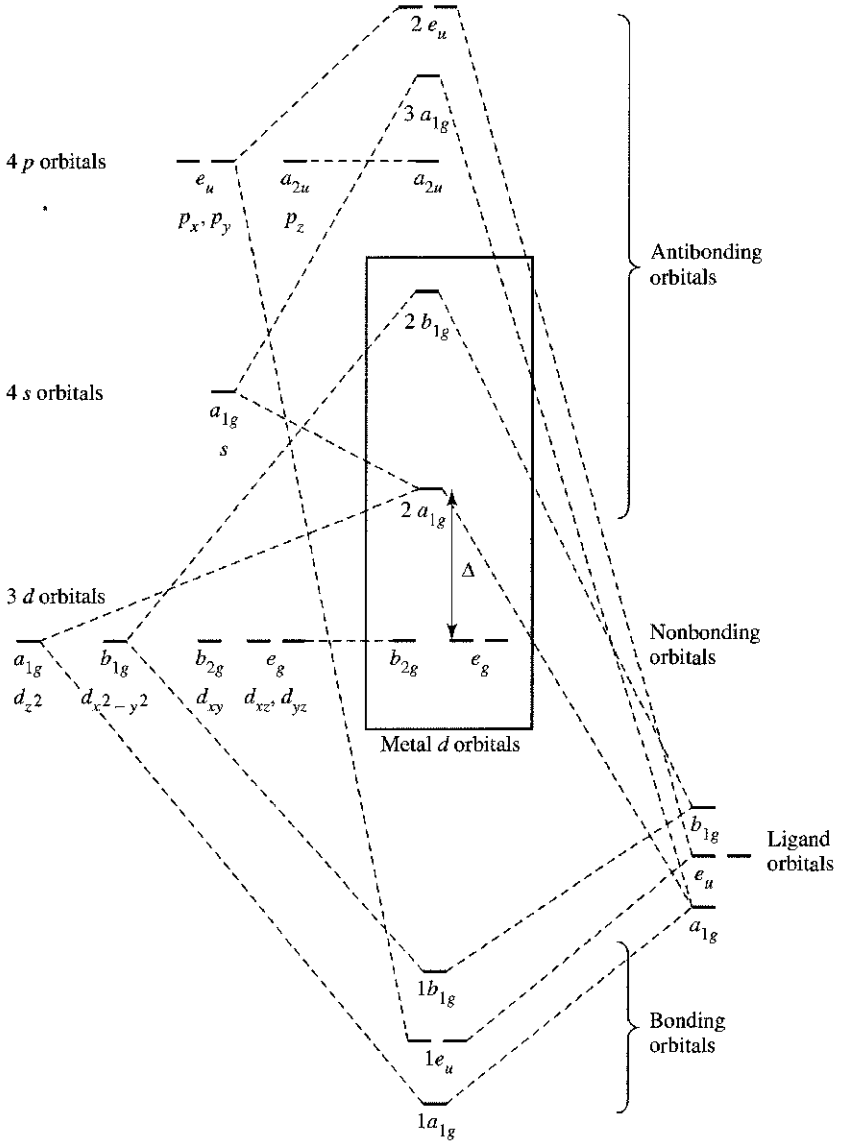

FIGURE 10-13 D_{4h} Molecular Orbitals (σ orbitals only). (Adapted from T. A. Albright, J. K. Burdett, and M.-Y. Whangbo, *Orbital Interactions in Chemistry*, Wiley-Interscience, New York, 1985, p. 296. © 1985, John Wiley & Sons, Inc. Reprinted by permission of John Wiley & Sons, Inc.)

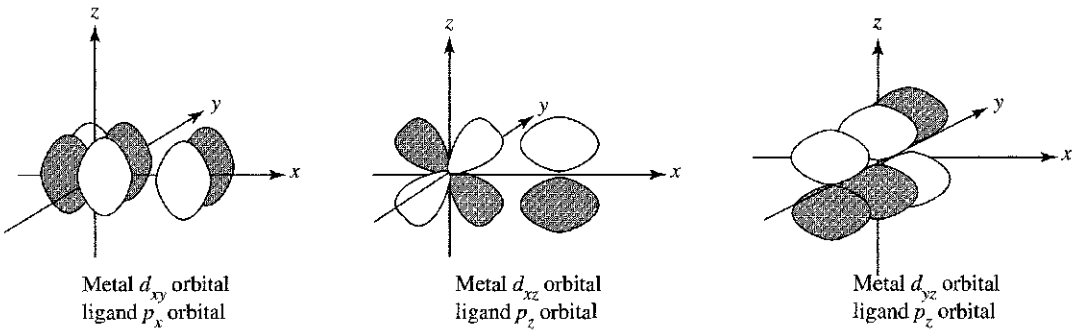

FIGURE 10-14 π-Bonding Orbitals in D_{4h} Molecules.

using relativistic corrections in the calculations. In all cases, there is, however, agreement that the b_{2g}, e_g, and a_{1g} orbitals are all low and have small differences in energy (from a few hundred to 12,600 cm^{-1}), and the b_{1g} orbital has a much higher energy (20,000 to more than 30,000 cm^{-1} above the next highest orbital). In the $[Pt(CN)_4]^{2-}$ ion, it is described as being higher in energy than the a_{2u} (mostly from the metal p_z).

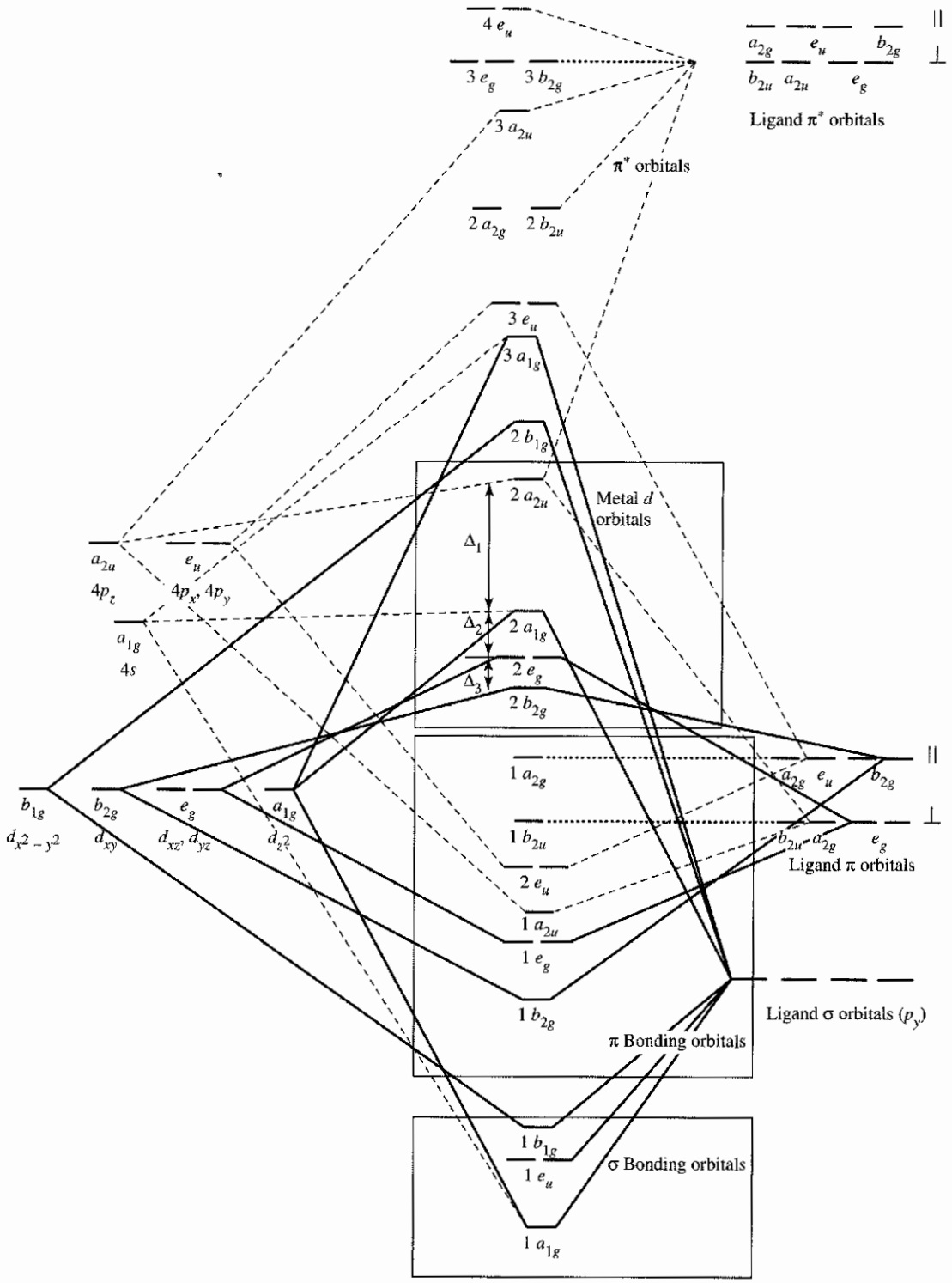

FIGURE 10-15 D_{4h} Molecular Orbitals, Including π Orbitals. Interactions with metal d orbitals are indicated by solid lines, interactions with metal s and p orbitals by dashed lines, and nonbonding orbitals by dotted lines.

The remaining high-energy orbitals are important only in excited states, and will not be considered further.

The important parts of this diagram are these major groups. Eight electrons from the ligands form the σ bonds, the next 16 electrons from the ligands can either π bond slightly or remain essentially nonbonding, and the remaining electrons from the metal ion occupy the third set. In the case of Ni^{2+} and Pt^{2+}, there are eight *d* electrons and there is a large gap in energy between their orbitals and the LUMO ($2a_{2u}$), leading to diamagnetic complexes. The effect of the π* orbitals of the ligand is to increase the difference in energy between these orbitals. For example, in $[PtCl_4]^{2-}$, with no π* orbitals, the difference between the $2e_g$ and $2a_{1g}$ orbitals is about 6000 cm^{-1} and the difference between the $2a_{1g}$ and $2a_{2u}$ orbitals is about 23,500 cm^{-1}. The corresponding differences for $[Pt(CN)_4]^{2-}$ are 12,600 and more than 30,000 cm^{-1}.[16]

The energy differences between the orbitals in this set are labeled Δ_1, Δ_2, and Δ_3 from top to bottom. Because b_{2g} and e_g are π orbitals, their energies will change significantly if the ligands are changed. We should also note that Δ_1 is related to Δ_o, is usually much larger than Δ_2 and Δ_3, and is almost always larger than Π, the pairing energy. This means that the b_{1g} or a_{2u} level, whichever is lower, is usually empty for metal ions with fewer than nine electrons.

10-3-6 TETRAHEDRAL COMPLEXES

Sigma bonding

The σ-bonding orbitals for tetrahedral complexes are easily determined on the basis of symmetry, using the coordinate system illustrated in Figure 10-16 to give the results in Table 10-10. The reducible representation includes the A_1 and T_2 irreducible representations, allowing for four bonding MOs. The energy level picture for the *d* orbitals is inverted from the octahedral levels, with *e* the nonbonding and t_2 the bonding and antibonding levels. In addition, the split (now called Δ_t) is smaller than for octahedral geometry; the general result is $\Delta_t = \frac{4}{9}\Delta_o$ (Figure 10-17).

Pi bonding

The π orbitals are more difficult to see, but if the *y* axis of the ligand orbitals is chosen along the bond axis and the *x* and *z* axes are arranged to allow the C_2 operation to work properly, the results in Table 10-10 are obtained. The reducible representation includes the *E*, T_1, and T_2 irreducible representations. The T_1 has no matching metal atom

TABLE 10-10
Representations of Tetrahedral Orbitals

T_d	E	$8C_3$	$3C_2$	$6S_4$	$6\sigma_d$		
A_1	1	1	1	1			$x^2 + y^2 + z^2$
A_2	1	−1	1	−1			
E	2	−1	2	0			$(2x^2 - x^2 - y^2, x^2 - y^2)$
T_1	3	0	−1	1		(R_x, R_y, R_z)	
T_2	3	0	−1	−1		(x, y, z)	(xy, yz, xz)
Γ_σ	4	1	0	0		$A_1 + T_2$	
Γ_π	8	−1	0	0		$E + T_1 + T_2$	

[16]H. B. Gray and C. J. Ballhausen, *J. Am. Chem. Soc.*, **1963**, *85*, 260.

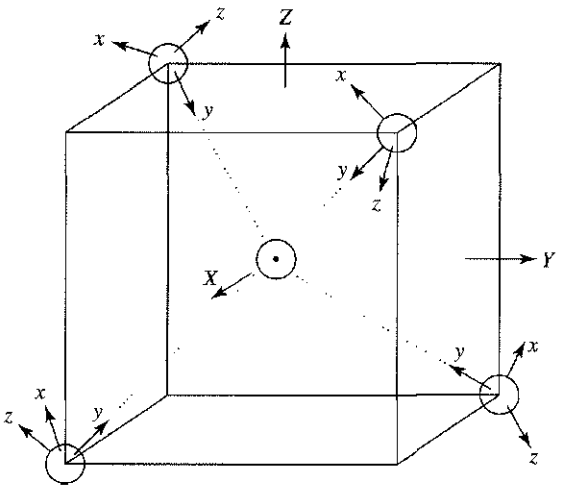

FIGURE 10-16 Coordinate System for Tetrahedral Orbitals.

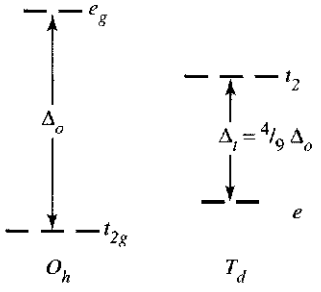

FIGURE 10-17 Orbital Splitting in Octahedral and Tetrahedral Geometries.

orbitals, E matches d_{z^2} and $d_{x^2-y^2}$, and T_2 matches d_{xy}, d_{xz}, and d_{yz}. The E and T_2 interactions lower the energy of the bonding orbitals, and raise the corresponding antibonding orbitals, for a net increase in Δ_t. An additional complication appears when both bonding and antibonding π orbitals are available on the ligand, as is true for CO or CN^-. Figure 10-18 shows the orbitals and their relative energies for $Ni(CO)_4$, in which the interactions of the CO σ and π orbitals with the metal orbitals are probably small. Much of the bonding is from M ⟶ L π bonding. In cases in which the d orbitals are not fully occupied, σ bonding is likely to be more important, with resulting shifts of the a_1 and t_2 orbitals to lower energies and the $4s$ and $4p$ orbitals to higher energies.

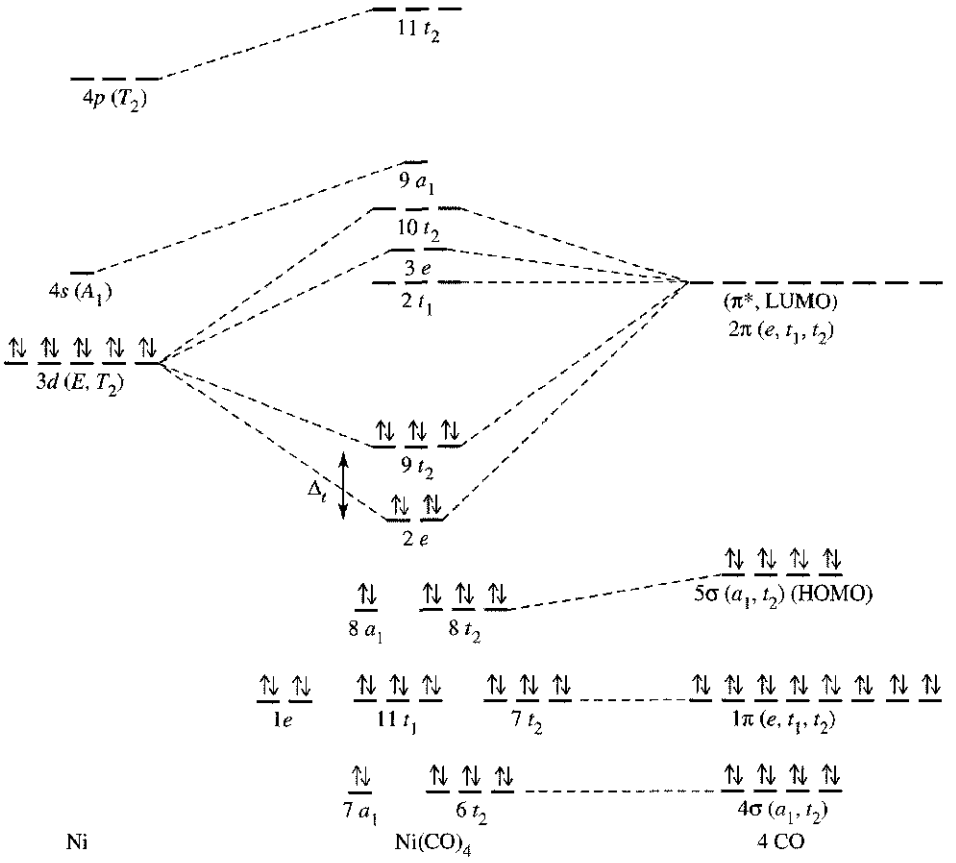

FIGURE 10-18 Molecular Orbitals for Tetrahedral $Ni(CO)_4$. C. W. Bauschlicher, Jr., and P. S. Bagus, *J. Chem. Phys.*, **1984**, *81*, 5889, argue that there is almost no σ bonding from the $4s$ and $4p$ orbitals of Ni, and that the d^{10} configuration is the best starting place for the calculations, as shown here. G. Cooper, K. H. Sze, and C. E. Brion, *J. Am. Chem. Soc.*, **1989**, *111*, 5051, include the metal $4s$ as a significant part of σ bonding, but with essentially the same net result in molecular orbitals.

10-4 ANGULAR OVERLAP

Although the formation of bonding orbitals is included in the description of the ligand field model, there is no explicit use of the energy change that results. In addition, the ligand field approach to energy levels in coordination complexes is more difficult to use when considering an assortment of ligands or structures with symmetry other than octahedral, square planar, or tetrahedral. A variation with the flexibility to deal with a variety of possible geometries and with a mixture of ligands is called the **angular overlap** model.[17,18] This approach estimates the strength of interaction between individual ligand orbitals and metal *d* orbitals based on the overlap between them and then combines these values for all ligands and all *d* orbitals for the complete picture. Both σ and π interactions are considered, and different coordination numbers and geometries can be treated. The term angular overlap is used because the amount of overlap depends strongly on the angles of the metal orbitals and the angle at which the ligand approaches.

In the angular overlap approach, the energy of a metal *d* orbital in a coordination complex is determined by summing the effects of each of the ligands on that orbital. Some ligands will have a strong effect on a particular *d* orbital, some a weaker effect, and some no effect at all, because of their angular dependence. Similarly, both σ and π interactions must be taken into account to determine the final energy of a particular orbital. By systematically considering each of the five *d* orbitals, we can use this approach to determine the overall energy pattern corresponding to the coordination geometry around the metal.

10-4-1 SIGMA-DONOR INTERACTIONS

The strongest σ interaction is between a metal d_z^2 orbital and a ligand *p* orbital (or a hybrid ligand orbital of the same symmetry), as shown in Figure 10-19. The strength of all other σ interactions is determined relative to the strength of this reference interaction. Interaction between these two orbitals results in a bonding orbital, which has a larger component of the ligand orbital, and an antibonding orbital, which is largely metal orbital in composition. Although the increase in energy of the antibonding orbital is larger than the decrease in energy of the bonding orbital, we will approximate the molecular orbital energies by an increase in the antibonding (mostly metal *d*) orbital of e_σ and a decrease in energy of the bonding (mostly ligand) orbital of e_σ.

Similar changes in orbital energy result from other interactions between metal *d* orbitals and ligand orbitals, with the magnitude dependent on the ligand location and the specific *d* orbital being considered. Table 10-11 gives values of these energy changes for a variety of shapes. Calculation of the numbers in the table (all in e_σ units) is beyond the

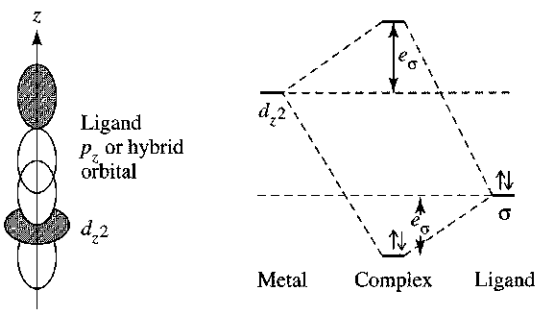

FIGURE 10-19 Sigma Interaction for Angular Overlap.

[17]E. Larsen and G. N. La Mar, *J. Chem. Educ.*, **1974**, *51*, 633. (Note: There are misprints on pp. 635 and 636.)

[18]J. K. Burdett, *Molecular Shapes*, Wiley-Interscience, New York, 1980.

TABLE 10-11
Angular Overlap Parameters: Sigma Interactions

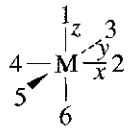

Octahedral positions

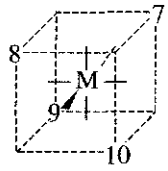

Tetrahedral positions

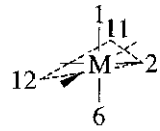

Trigonal-bipyramidal positions

CN	*Shape*	*Positions*
2	Linear	1, 6
3	Trigonal	2, 11, 12
3	T shape	1, 3, 5
4	Tetrahedral	7, 8, 9, 10
4	Square planar	2, 3, 4, 5
5	Trigonal bipyramidal	1, 2, 6, 11, 12
5	Square pyramidal	1, 2, 3, 4, 5
6	Octahedral	1, 2, 3, 4, 5, 6

Sigma Interactions (all in units of e_σ)
Metal d Orbital

Ligand Position	z^2	$x^2 - y^2$	xy	xz	yz
1	1	0	0	0	0
2	$\frac{1}{4}$	$\frac{3}{4}$	0	0	0
3	$\frac{1}{4}$	$\frac{3}{4}$	0	0	0
4	$\frac{1}{4}$	$\frac{3}{4}$	0	0	0
5	$\frac{1}{4}$	$\frac{3}{4}$	0	0	0
6	1	0	0	0	0
7	0	0	$\frac{1}{3}$	$\frac{1}{3}$	$\frac{1}{3}$
8	0	0	$\frac{1}{3}$	$\frac{1}{3}$	$\frac{1}{3}$
9	0	0	$\frac{1}{3}$	$\frac{1}{3}$	$\frac{1}{3}$
10	0	0	$\frac{1}{3}$	$\frac{1}{3}$	$\frac{1}{3}$
11	$\frac{1}{4}$	$\frac{3}{16}$	$\frac{9}{16}$	0	0
12	$\frac{1}{4}$	$\frac{3}{16}$	$\frac{9}{16}$	0	0

scope of this book, but the reader should be able to justify the numbers qualitatively by comparing the amount of overlap between the orbitals being considered.

The angular overlap approach is best described by example. We will consider first the most common geometry for coordination complexes, octahedral.

EXAMPLE

$[M(NH_3)_6]^{n+}$ $[M(NH_3)_6]^{n+}$ ions are examples of octahedral complexes with only σ interactions. The ammonia ligands have no π orbitals available, either of donor or acceptor character, for bonding with the metal ion. The lone pair orbital is mostly nitrogen p_z orbital in composition, and the other p orbitals are used in bonding to the hydrogens (see Figure 5-31).

In calculating the orbital energies in a complex, the value for a given d orbital is the sum of the numbers for the appropriate ligands in the vertical column for that orbital in Table 10-11. The change in energy for a specific ligand orbital is the sum of the numbers for all d orbitals in the horizontal row for the required ligand position.

Metal *d* Orbitals d_{z^2} orbital: The interaction is strongest with ligands in positions 1 and 6, along the z axis. Each interacts with the orbital to raise its energy by e_σ. The ligands in positions 2, 3, 4, and 5 interact more weakly with the d_{z^2} orbital, each raising the energy of the orbital by $\frac{1}{4}\,e_\sigma$. Overall, the energy of the d_{z^2} orbital is increased by the sum of all these interactions, for a total of $3e_\sigma$.

$d_{x^2-y^2}$ orbital: The ligands in positions 1 and 6 do not interact with this metal orbital. However, the ligands in positions 2, 3, 4, and 5 each interact to raise the energy of the metal orbital by $\frac{3}{4}\,e_\sigma$, for a total increase of $3e_\sigma$.

d_{xy}, d_{xz}, and d_{yz} orbitals: None of these orbitals interact in a sigma fashion with any of the ligand orbitals, so the energy of these metal orbitals remains unchanged.

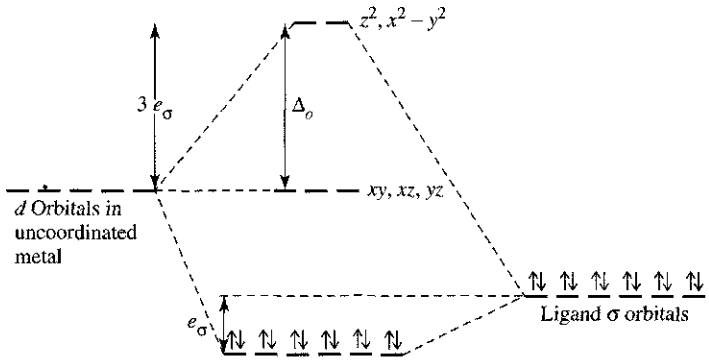

FIGURE 10-20 Energies of *d* Orbitals in Octahedral Complexes: Sigma-Donor Ligands. $\Delta_o = 3e_\sigma$. Metal *s* and *p* orbitals also contribute to the bonding molecular orbitals.

Ligand Orbitals The energy changes for the ligand orbitals are the same as those above for each interaction. The totals, however, are taken *across a row* of the Table 10-11, including each of the *d* orbitals.

Ligands in positions 1 and 6 interact strongly with d_{z^2} and are lowered by e_σ. They do not interact with the other *d* orbitals.

Ligands in positions 2, 3, 4, and 5 are lowered by $\frac{1}{4}\, e_\sigma$ by interaction with d_{z^2} and by $\frac{3}{4}\, e_\sigma$ by interaction with $d_{x^2-y^2}$, for a total of e_σ.

Overall, each ligand orbital is lowered by e_σ.

The resulting energy pattern is also shown in Figure 10-20. This result is the same as the pattern obtained from the ligand field approach. Both describe how the metal complex is stabilized: as two of the *d* orbitals of the metal increase in energy and three remain unchanged, the six ligand orbitals fall in energy, and electron pairs in those orbitals are stabilized in the formation of ligand-metal bonds. The net stabilization is $12e_\sigma$ for the bonding pairs; any *d* electrons in the upper (e_g) level are destabilized by $3e_\sigma$ each.

The more complete MO picture that includes use of the metal *s* and *p* orbitals in the formation of the bonding MOs and the four additional antibonding orbitals was shown in Figure 10-5. There are no examples of complexes with electrons in the antibonding orbitals from *s* and *p* orbitals, and these high-energy antibonding orbitals are not significant in describing the spectra of complexes, so we will not consider them further.

EXERCISE 10-8

Using the angular overlap model, determine the relative energies of *d* orbitals in a metal complex of formula ML_4 having tetrahedral geometry. Assume that the ligands are capable of σ interactions only.

How does this result for Δ_t compare with the value for Δ_o?

10-4-2 PI-ACCEPTOR INTERACTIONS

Ligands such as CO, CN^-, and phosphines (of formula PR_3) are π acceptors, with empty orbitals that can interact with metal *d* orbitals in a π fashion. In the angular overlap model, the strongest π interaction is considered to be between a metal d_{xz} orbital and a ligand π* orbital, as shown in Figure 10-21. Because the ligand π* orbitals are higher in energy than the original metal *d* orbitals, the resulting bonding MOs are lower in energy than the metal *d* orbitals (a difference of e_π) and the antibonding MOs are higher in energy. The *d* electrons then occupy the bonding MO, with a net energy change of $-4e_\pi$ for each electron, as in Figure 10-22.

Because the overlap for these orbitals is smaller than the σ overlap described in the previous section, $e_\pi < e_\sigma$. The other π interactions are weaker than this reference interaction, with the magnitudes depending on the degree of overlap between the orbitals. Table 10-12 gives values for ligands at the same angles as in Table 10-11.

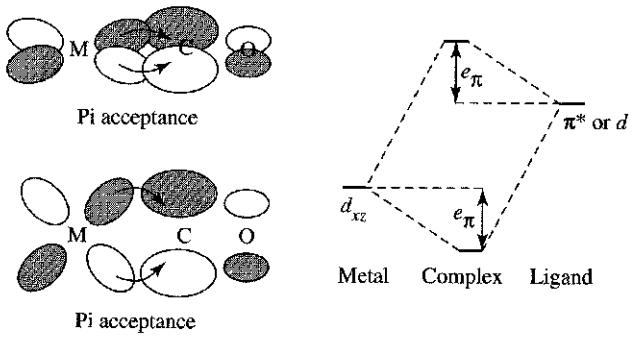

FIGURE 10-21 Pi-Acceptor Interactions.

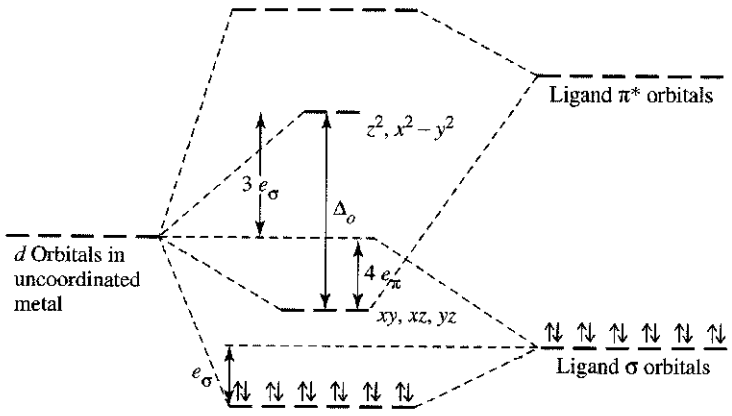

FIGURE 10-22 Energies of d Orbitals in Octahedral Complexes: Sigma-Donor and Pi-Acceptor Ligands. $\Delta_o = 3e_\sigma + 4e_\pi$. Metal s and p orbitals also contribute to the bonding molecular orbitals.

TABLE 10-12
Angular Overlap Parameters: Pi Interactions

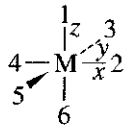

Octahedral positions

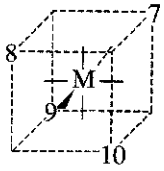

Tetrahedral positions

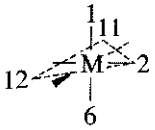

Trigonal bipyramidal positions

CN	*Shape*	*Positions*
2	Linear	1, 6
3	Trigonal	2, 11, 12
3	T shape	1, 3, 5
4	Tetrahedral	7, 8, 9, 10
4	Square planar	2, 3, 4, 5
5	Trigonal bipyramidal	1, 2, 6, 11, 12
5	Square pyramidal	1, 2, 3, 4, 5
6	Octahedral	1, 2, 3, 4, 5, 6

Pi Interactions (all in units of e_π)
Metal d Orbital

Ligand Position	z^2	$x^2 - y^2$	xy	xz	yz
1	0	0	0	1	1
2	0	0	1	1	0
3	0	0	1	0	1
4	0	0	1	1	0
5	0	0	1	0	1
6	0	0	0	1	1
7	$\frac{2}{3}$	$\frac{2}{3}$	$\frac{2}{9}$	$\frac{2}{9}$	$\frac{2}{9}$
8	$\frac{2}{3}$	$\frac{2}{3}$	$\frac{2}{9}$	$\frac{2}{9}$	$\frac{2}{9}$
9	$\frac{2}{3}$	$\frac{2}{3}$	$\frac{2}{9}$	$\frac{2}{9}$	$\frac{2}{9}$
10	$\frac{2}{3}$	$\frac{2}{3}$	$\frac{2}{9}$	$\frac{2}{9}$	$\frac{2}{9}$
11	0	$\frac{3}{4}$	$\frac{1}{4}$	$\frac{1}{4}$	$\frac{3}{4}$
12	0	$\frac{3}{4}$	$\frac{1}{4}$	$\frac{1}{4}$	$\frac{3}{4}$

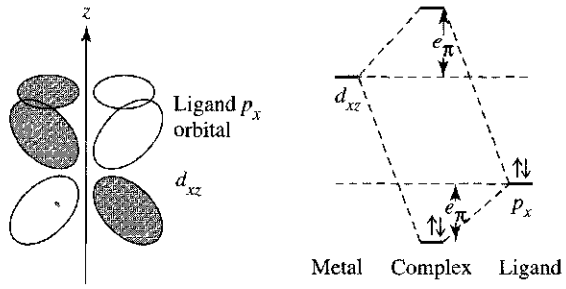

FIGURE 10-23 Pi-Donor Interactions.

EXAMPLE

$[M(CN)_6]^{n-}$ The result of these interactions for $[M(CN)_6]^{n-}$ complexes is shown in Figure 10-22. The d_{xy}, d_{xz}, and d_{yz} orbitals are lowered by $4e_\pi$ each and the six ligand positions have an average increase in orbital energy of $2e_\pi$. The resulting ligand π^* orbitals have high energies and are not involved directly in the bonding. The net value of the t_{2g}-e_g split is $\Delta_o = 3e_\sigma + 4e_\pi$.

10-4-3 PI-DONOR INTERACTIONS

The interactions between occupied ligand *p*, *d*, or π^* orbitals and metal *d* orbitals are similar to those in the π-acceptor case. In other words, the angular overlap model treats π-donor ligands similarly to π-acceptor ligands except that *for π-donor ligands, the signs of the changes in energy are reversed*, as shown in Figure 10-23. The metal *d* orbitals are raised in energy, whereas the ligand π orbitals are lowered in energy. The overall effect is shown in Figure 10-24.

EXAMPLE

$[MX_6]^{n-}$ Halide ions donate electron density to a metal via p_y orbitals, a σ interaction; the ions also have p_x and p_z orbitals that can interact with metal orbitals and donate additional electron density via π interactions. We will use $[MX_6]^{n-}$ as our example, where X is a halide ion or other ligand that is both a σ and a π donor.

d_{z^2} and $d_{x^2-y^2}$ orbitals: Neither of these orbitals has the correct orientation for π interactions; therefore, the π orbitals have no effect on the energies of these *d* orbitals.

d_{xy}, d_{xz}, and d_{yz} orbitals: Each of these orbitals interacts in a π fashion with four of the ligands. For example, the d_{xy} orbital interacts with ligands in positions 2, 3, 4, and 5 with a

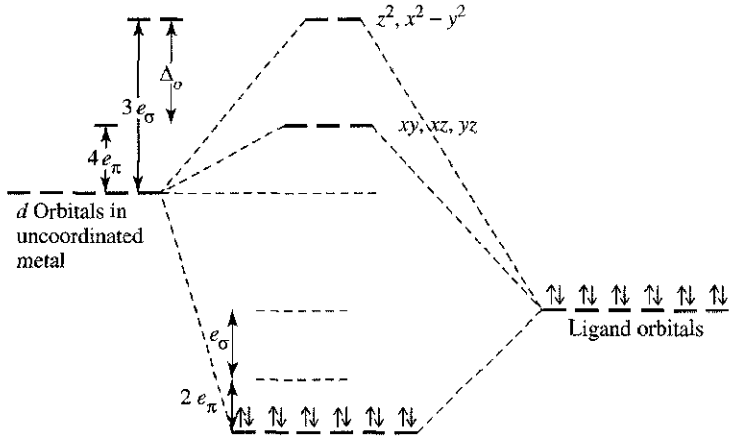

FIGURE 10-24 Energies of *d* Orbitals in Octahedral Complexes: Sigma-Donor and Pi-Donor Ligands. $\Delta_o = 3e_\sigma - 4e_\pi$. Metal *s* and *p* orbitals also contribute to the bonding molecular orbitals.

strength of $1e_\pi$, resulting in a total increase of the energy of the d_{xy} orbital of $4e_\pi$ (the interaction with ligands at positions 1 and 6 is zero). The reader should verify by using Table 10-12 that the d_{xz} and d_{yz} orbitals are also raised in energy by $4e_\pi$.

The overall effect on the energies of the d orbitals of the metal, including both σ and π donor interactions, is shown in Figure 10-24.

EXERCISE 10-9

Using the angular overlap model, determine the splitting pattern of d orbitals for a tetrahedral complex of formula MX_4, where X is a ligand that can act as σ donor and π donor.

In general, in situations involving ligands that can behave as both π acceptors and π donors (such as CO and CN^-), the π-acceptor nature predominates. Although π-donor ligands cause the value of Δ_o to decrease, the larger effect of the π-acceptor ligands cause Δ_o to increase. Pi-acceptor ligands are better at splitting the d orbitals (causing larger changes in Δ_o).

EXERCISE 10-10

Determine the energies of the d orbitals predicted by the angular overlap model for a square-planar complex:

a. Considering σ interactions only.

b. Considering both σ-donor and π-acceptor interactions.

10-4-4 TYPES OF LIGANDS AND THE SPECTROCHEMICAL SERIES

Ligands are frequently classified by their donor and acceptor capabilities. Some, like ammonia, are σ donors only, with no orbitals of appropriate symmetry for π bonding. Bonding by these ligands is relatively simple, using only the σ orbitals identified in Figure 10-4. The ligand field split, Δ, then depends on the relative energies of the metal ion and ligand orbitals and on the degree of overlap. Ethylenediamine has a stronger effect than ammonia among these ligands, generating a larger Δ. This is also the order of their proton basicity:

$$\text{en} > NH_3$$

The halide ions have ligand field strengths in the order

$$F^- > Cl^- > Br^- > I^-$$

which is also the order of proton basicity of these ligands.

Ligands that have occupied p orbitals are potentially π donors. They tend to donate these electrons to the metal along with the σ-bonding electrons. As shown in Section 10-4-3, this π-donor interaction decreases Δ. As a result, most halide complexes have high-spin configurations. Other primarily σ-donor ligands that can also act as π donors include H_2O, OH^-, and RCO_2^-. They fit into the series in the order

$$H_2O > F^- > RCO_2^- > OH^- > Cl^- > Br^- > I^-$$

with OH^- below H_2O in the series because it has more π-donating tendency.

When ligands have vacant π^* or d orbitals, there is the possibility of π back-bonding, and the ligands are π acceptors. This addition to the bonding scheme increases Δ. Ligands that do this very effectively include CN^-, CO, and many others. A selected list of these ligands in order is

$$CO, CN^- > \text{phenanthroline (phen)} > NO_2^- > NCS^-$$

When the two lists of ligands are combined, thiocyanate turns out to have a smaller effect than ammonia. This list is called the **spectrochemical series** and runs roughly in order from strong π-acceptor effect to strong π-donor effect:

$$CO, CN^- > \text{phen} > NO_2^- > \text{en} > NH_3 > NCS^- > H_2O > F^- > RCO_2^- > OH^- > Cl^- > Br^- > I^-$$

Low spin		High spin
Strong field		Weak field
Large Δ		Small Δ
π acceptors	σ donor only	π donors

Many of the large number of other ligands possible could be included in such a list, but because the effects are changed by other circumstances (different metal ion, different charge on the metal, other ligands also present), attempting to put a large number of ligands in such a list is not generally helpful.

10-4-5 MAGNITUDES OF e_σ, e_π, AND Δ

Changing the ligand or the metal changes the magnitude of e_σ and e_π, with resulting changes in Δ and a possible change in the number of unpaired electrons. For example, water is a relatively weak-field ligand. When combined with Co^{2+} in an octahedral geometry, the result is a high-spin complex with three unpaired electrons. Combined with Co^{3+}, water gives a low-spin complex with no unpaired electrons. The increase in charge on the metal changes Δ_o sufficiently to favor low spin, as shown in Figure 10-25.

Similar effects appear with different ligands. $[Fe(H_2O)_6]^{3+}$ is a high-spin species, and $[Fe(CN)_6]^{3-}$ is low-spin. Replacing H_2O with CN^- is enough to favor low spin and, in this case, the change in Δ_o is caused solely by the ligand. As described in Section 10-3, the balance between Δ, Π_c and Π_e (the Coulombic and exchange energies) determines whether a specific complex will be high or low spin. Because Δ_t is small, low-spin tetrahedral complexes are unlikely; ligands with strong enough fields to give low-spin complexes are likely to form low-spin octahedral complexes instead.

Tables 10-13 and 10-14 show values for some angular overlap parameters derived from electronic spectra. Several trends can be seen in these data. First, e_σ is always larger than e_π, in some cases by a factor as large as 9, in others less than 2. This is as expected, because the σ interaction is based on overlap on the line through the nuclei, along which the ligand orbital extends, whereas the π interaction has smaller overlap because the interacting orbitals are not directed toward each other. In addition, the magnitudes of both the σ and π parameters decrease with increasing size and decreasing electronegativity of the halide ions. Increasing the size of the ligand and the corresponding bond length leads to a smaller overlap with the metal d orbitals. In addition, decreasing the electronegativity decreases the pull that the ligand exerts on the metal d electrons, so the two effects reinforce each other.

In Table 10-13, ligands in each group are listed in their order in the spectrochemical series. For example, for octahedral complexes of Cr^{3+}, CN^- is listed first; it is the

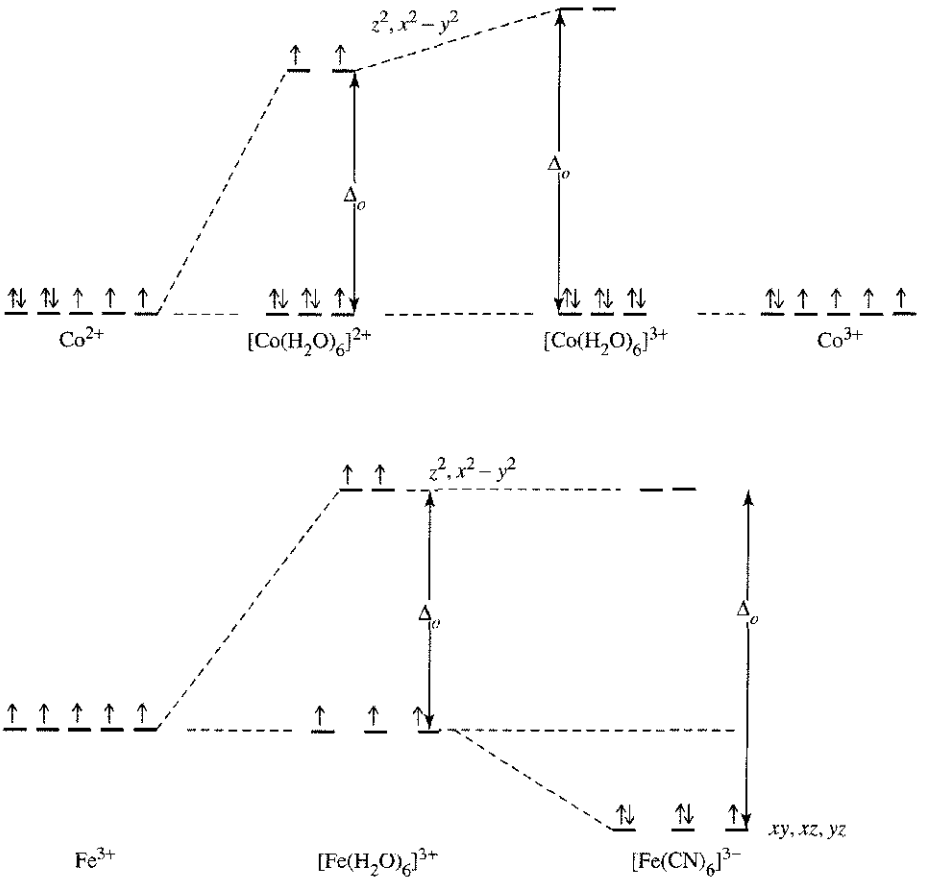

FIGURE 10-25
$[Co(H_2O)_6]^{2+}$, $[Co(H_2O)_6]^{3+}$, $[Fe(H_2O)_6]^{3+}$, $[Fe(CN)_6]^{3-}$ and Unpaired Electrons.

highest in the spectrochemical series and is a π acceptor (e_π is negative). Ethylenediamine and NH_3 are next, listed in order of their e_σ values (which measure σ-donor ability). The halide ions are π donors as well as σ donors and are at the bottom of the series.

Comparison of Pa(IV) and U(V), which are isoelectronic, shows that increasing the metal's nuclear charge increases both the σ and π parameters while retaining approximately the same ratio between them, again an expected result from drawing the ligands in closer to the metal nucleus.

Some measures of orbital interaction show different results. For example, these parameters derived from spectra show the order of interaction as $F^- > Cl^- > Br^-$, whereas the reverse is predicted on the basis of donor ability. This can be rationalized as resulting from measurements influenced by different orbitals. The spectral data are derived from transitions to antibonding orbitals; other measures may be derived from bonding molecular orbitals. In addition, the detailed calculation of the energies of the molecular orbitals shows that the antibonding orbital energy is more strongly influenced by the ligand orbitals, but the bonding orbital energy is more strongly influenced by the metal orbitals.[19] The magnitude of the antibonding effect is larger.

Special cases

The angular overlap model can describe the electronic energy of complexes with different shapes or with combinations of different ligands. It is possible to estimate approximately the magnitudes of e_σ and e_π with different ligands and to predict the effects on the electronic structure of complexes such as $[Co(NH_3)_4Cl_2]^+$. This complex, like nearly all

[19] J. K. Burdett, *Molecular Shapes*, Wiley-Interscience, New York, 1980, p. 157.

TABLE 10-13
Angular Overlap Parameters

Metal	*X*	$e_\sigma\ (cm^{-1})$	$e_\pi\ (cm^{-1})$	$\Delta_o = 3e_\sigma - 4e_\pi$	$\Delta\sigma\ (cm^{-1})$
Octahedral MX_6 complexes					
Cr^{3+}	CN^-	7530	−930	26,310	
	en	7260		21,780	
	NH_3	7180		21,540	
	H_2O	7550	1850	15,250	
	F^-	8200	2000	16,600	
	Cl^-	5700	980	13,180	
	Br^-	5380	950	12,340	
	I^-	4100	670	620	
Ni^{2+}	en	4000			
	NH_3	3600			
$M(NH_3)_5X$ complexes					
Cr(III)	CN^-				1310
	OH^-	8670	3000		
	NH_3	7030	0		
	H_2O	7900			−1100
	NCS^-				−1000
	F^-	7390	1690		−1410
	Cl^-	5540	1160		−2120
	Br^-	4920	830		−2510
	I^-				−2970
	py	5850	−670		
Pa(IV)	F^-	2870	1230		
	Cl^-	1264	654		
	Br^-	976	683		
	I^-	725	618		
U(V)	F^-	4337	1792		
	Cl^-	2273	1174		
	Br^-	1775	1174		

SOURCE: MX_6 data from B. N. Figgis and M. A. Hitchman, *Ligand Field Theory and Its Applications*, Wiley-VCH, New York, 2000, p. 71, and references therein; $M(NH_3)_5X$ data adapted from J. K. Burdett, *Molecular Shapes*, Wiley-Interscience, New York, 1980, p. 153, with permission.

NOTE: $\Delta\sigma = e_\sigma(NH_3) - e_\sigma(X)$, the difference in energy between the b_1 $(d_{x^2-y^2})$ and the a_1 (d_{z^2}) orbitals, determined by the difference between two spectral bands.

Co(III) complexes except $[CoF_6]^{3-}$ and $[Co(H_2O)_3F_3]$, is low spin, so the magnetic properties do not depend on Δ_o. However, the magnitude of Δ_o does have a significant effect on the visible spectrum, as discussed in Chapter 11. Angular overlap can be used to help compare the energies of different geometries—for example, to predict whether a four-coordinate complex is likely to be tetrahedral or square planar, as described in Section 10-6. It is also possible to use the angular overlap model to estimate the energy change for reactions in which the transition state results in either a higher or lower coordination number, as described in Chapter 12.

10-5 THE JAHN-TELLER EFFECT

The Jahn-Teller theorem[20] states that there cannot be unequal occupation of orbitals with identical energies. To avoid such unequal occupation, the molecule distorts so that these orbitals are no longer degenerate. For example, octahedral Cu(II), a d^9 ion, would have three electrons in the two e_g levels without the Jahn-Teller effect, as in the

[20]H. A. Jahn and E. Teller, *Proc. R. Soc. London*, **1937**, *A161*, 220.

TABLE 10-14
Angular Overlap Parameters for MA_4B_2 Complexes

	Equatorial Ligands (A)			*Axial Ligands (B)*			*Reference*
		$e_\sigma\ (cm^{-1})$	$e_\pi\ (cm^{-1})$		$e_\sigma\ (cm^{-1})$	$e_\pi\ (cm^{-1})$	
Cr^{3+}, D_{4h}	en	7233	0	F^-	7811	2016	a
		7233		F^-	8033	2000	c
		7333		Cl^-	5558	900	a
		7500		Cl^-	5857	1040	c
		7567		Br^-	5341	1000	a
		7500		Br^-	5120	750	c
		6987		I^-	4292	594	b
		6840		OH^-	8633	2151	a
		7490		H_2O	7459	1370	a
		7833		H_2O	7497	1410	c
		7534		dmso	6769	1653	b
	H_2O	7626	1370 (assumed)	F^-	8510	2539	a
	NH_3	6967	0	F^-	7453	1751	a
Ni^2, D_{4h}							
	py	4670	570	Cl^-	2980	540	c
		4500	500	Br^-	2540	340	c
	pyrazole	5480	1370	Cl^-	2540	380	c
		5440	1350	Br^-	1980	240	c
$[CuX_4]^{2-}$, D_{2d}							
	Cl^-	6764	1831				c
	Br^-	4616	821				c

SOURCE: [a] M. Keeton, B. Fa-chun Chou, and A. B. P. Lever, *Can. J. Chem.* **1971**, *49*, 192; erratum, *ibid.*, **1973**, *51*, 3690.
[b] T. J. Barton and R. C. Slade, *J. Chem. Soc. Dalton Trans.*, **1975**, 650.
[c] M. Gerloch and R. C. Slade, *Ligand Field Parameters*, Cambridge University Press, London, 1973, p. 186.

center of Figure 10-26. The Jahn-Teller effect requires that the shape of the complex change slightly, resulting in a change in the energies of the orbitals. The resulting distortion is most often an elongation along one axis, but compression along one axis is also possible. In octahedral complexes, where the e_g orbitals are directed toward the ligands, distortion of the complex has a larger effect on these energy levels and a smaller effect when the t_{2g} orbitals are involved. The effect of both elongation and compression on *d* orbital energies is shown in Figure 10-26, and the expected Jahn-Teller effects are summarized in the following table:

Number of electrons	1	2	3	4	5	6	7	8	9	10
High-spin Jahn-Teller	w	w		s		w	w		s	
Low-spin Jahn-Teller	w	w		w	w		s		s	

w = weak Jahn-Teller effect expected (t_{2g} orbitals unevenly occupied); s = strong Jahn-Teller effect expected (e_g orbitals unevenly occupied); No entry = no Jahn-Teller effect expected.

EXERCISE 10-11

Using the usual *d*-orbital splitting diagrams, show that the Jahn-Teller effects in the table match the description in the preceding paragraph.

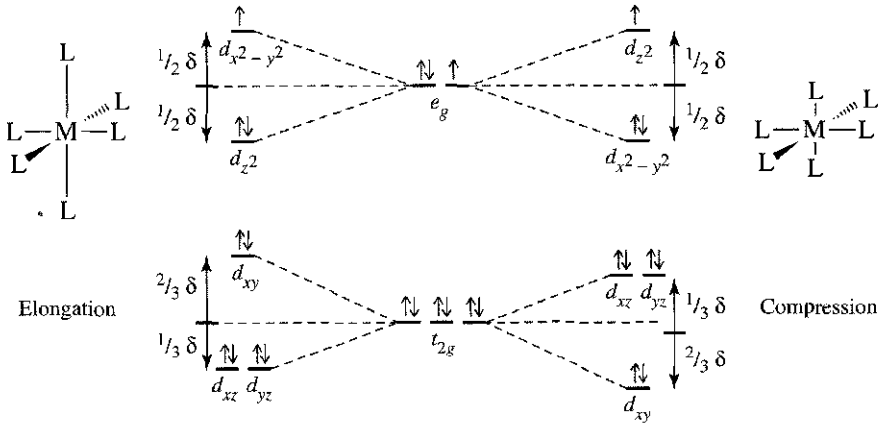

FIGURE 10-26 Jahn-Teller Effect on a d^9 Complex. Elongation along the z axis is coupled to a slight decrease in bond length for the other four bonding directions. Similar changes in energy result when the axial ligands have shorter bond distances. The resulting splits are larger for the e_g orbitals than for the t_{2g}. The energy differences are exaggerated in this figure.

Examples of significant Jahn-Teller effects are found in complexes of Cr(II) (d^4), high-spin Mn(III) (d^4), and Cu(II) (d^9). Ni(III) (d^7), and low-spin Co(II) (d^7) should also show this effect, but NiF_6^{3-} is the only known example for these metal ions. It has a distorted structure consistent with the Jahn-Teller theorem.

Low-spin Cr(II) complexes are octahedral with tetragonal distortion (distorted from O_h to D_{4h} symmetry). They show two absorption bands, one in the visible and one in the near-infrared region, caused by this distortion. In a pure octahedral field, there should be only one *d-d* transition (see Chapter 11 for more details). Cr(II) also forms dimeric complexes with Cr—Cr bonds in many complexes. The acetate, $Cr_2(OAc)_4$, is an example in which the acetate ions bridge between the two chromiums, with significant Cr—Cr bonding resulting in a nearly diamagnetic complex.

Curiously, the $[Mn(H_2O)_6]^{3+}$ ion appears to form an undistorted octahedron in $CsMn(SO_4)_2 \cdot 12\,H_2O$, although other Mn(III) complexes show the expected distortion.[21, 22]

Cu(II) forms the most common complexes with significant Jahn-Teller effects. In most cases, the distortion is an elongation of two bonds, but K_2CuF_4 forms a crystal with two shortened bonds in the octahedron. Elongation also plays a part in the change in equilibrium constants for complex formation. For example, $[Cu(NH_3)_4]^{2+}$ is readily formed in aqueous solution as a distorted octahedron with two water molecules at larger distances than the ammonias, but liquid ammonia is required for formation of the hexammine complex. The formation constants for these reactions show the difficulty of putting the fifth and sixth ammonias on the metal.[23] Which factor is the cause and which the result is uncertain, but the bond distances for the two axial positions are longer than those of the four equatorial positions, and the equilibrium constants are much smaller.

$$[Cu(H_2O)_6]^{2+} + NH_3 \rightleftharpoons [Cu(NH_3)(H_2O)_5]^{2+} + H_2O \qquad K_1 = 2 \times 10^4$$

$$[Cu(NH_3)(H_2O)_5]^{2+} + NH_3 \rightleftharpoons [Cu(NH_3)_2(H_2O)_4]^{2+} + H_2O \qquad K_2 = 4 \times 10^3$$

$$[Cu(NH_3)_2(H_2O)_4]^{2+} + NH_3 \rightleftharpoons [Cu(NH_3)_3(H_2O)_3]^{2+} + H_2O \qquad K_3 = 1 \times 10^3$$

$$[Cu(NH_3)_3(H_2O)_3]^{2+} + NH_3 \rightleftharpoons [Cu(NH_3)_4(H_2O)_2]^{2+} + H_2O \qquad K_4 = 2 \times 10^2$$

$$[Cu(NH_3)_4(H_2O)_2]^{2+} + NH_3 \rightleftharpoons [Cu(NH_3)_5(H_2O)]^{2+} + H_2O \qquad K_5 = 3 \times 10^{-1}$$

$$[Cu(NH_3)_5(H_2O)]^{2+} + NH_3 \rightleftharpoons [Cu(NH_3)_6]^{2+} + H_2O \qquad K_6 = \text{very small}$$

[21] A. Avdeef, J. A. Costamagna, and J. P. Fackler, Jr., *Inorg. Chem.*, **1974**, *13*, 1854.

[22] J. P. Fackler, Jr., and A. Avdeef, *Inorg. Chem.*, **1974**, *13*, 1864.

[23] R. M. Smith and A. E. Martell, *Critical Stability Constants, Vol. 4, Inorganic Complexes*, Plenum Press, New York, 1976, p. 41.

In many cases, Cu(II) complexes have square-planar or nearly square-planar geometry, with nearly tetrahedral shapes also possible. $[CuCl_4]^{2-}$, in particular, shows structures ranging from tetrahedral through square planar to distorted octahedral, depending on the cation present.[24]

10-6 FOUR- AND SIX-COORDINATE PREFERENCES

Angular overlap calculations of the energies expected for different numbers of *d* electrons and different geometries can give us some indication of relative stabilities. Here, we will consider the three major geometries, octahedral, square planar, and tetrahedral. In Chapter 12, similar calculations will be used to help describe reactions at the coordination sites.

Figure 10-27 shows the results of angular overlap calculations for d^0 through d^{10} electron configurations. Figure 10-27(a) compares octahedral and square-planar geometries. Because of the larger number of bonds formed in the octahedral complexes, they are more stable (lower energy) for all configurations except d^8, d^9, and d^{10}. A low-spin square-planar geometry has the same net energy as either a high- or low-spin octahedral geometry for all three of these configurations. This indicates that these configurations are the most likely to have square-planar structures, although octahedral is equally probable from this approach.

Figure 10-27(b) compares square-planar and tetrahedral structures. For strong-field ligands, square planar is preferred in all cases except d^0, d^1, d^2, and d^{10}. In those cases, the angular overlap approach predicts that the two structures are equally probable. For weak-field ligands, tetrahedral and square-planar structures also have equal energies in the d^5, d^6, and d^7 cases.

How accurate are these predictions? Their success is variable, because there are other differences between metals and between ligands. In addition, bond lengths for the same ligand-metal pair depend on the geometry of the complex. One factor that must be included in addition to the *d* electron energies is the interaction of the *s* and *p* orbitals of the metal with the ligand orbitals. The bonding orbitals from these interactions are at a lower energy than those from *d* orbital interactions and are therefore completely filled. Their overall energy is, then, a combination of the energy of the metal atomic orbitals (approximated by their orbital potential energies) and the ligand orbitals. Orbital potential energies for transition metals become more negative with increasing atomic number. As a result, the formation enthalpy for complexes also becomes more negative with increasing atomic number and increasing ionization energy. This trend provides a downward slope to the baseline under the contributions of the *d* orbital-ligand interactions shown in Figure 10-27(a). Burdett[25] has shown that the calculated values of enthalpy of hydration can reproduce the experimental values for enthalpy of hydration very well by using this technique. Figure 10-28 shows a simplified version of this, simply adding $-0.3e_\sigma$ (an arbitrary choice) to the total enthalpy for each increase in *Z* (which equals the number of *d* electrons). The parallel lines show this slope running through the d^0, d^5, and d^{10} points. Addition of a *d* electron beyond a completed spin set increases the hydration enthalpy until the next set is complete. Comparison with Figure 10-7, in which the experimental values are given, shows that the approach is at least approximately valid. Certainly other factors need to be included for complete agreement with experiment, but their influence seems small.

As expected from the values shown in Figure 10-27, Cu(II) (d^9) complexes show great variability in geometry. Complicating the simple picture used in this section is the change in bond distance that accompanies change in geometry. Overall, the two regular

[24]N. N. Greenwood and A. Earnshaw, *Chemistry of the Elements*, Pergamon Press, Elmsford, NY, 1984, pp. 1385–1386.

[25]J. K. Burdett, *J. Chem. Soc. Dalton Trans.*, **1976**, 1725.

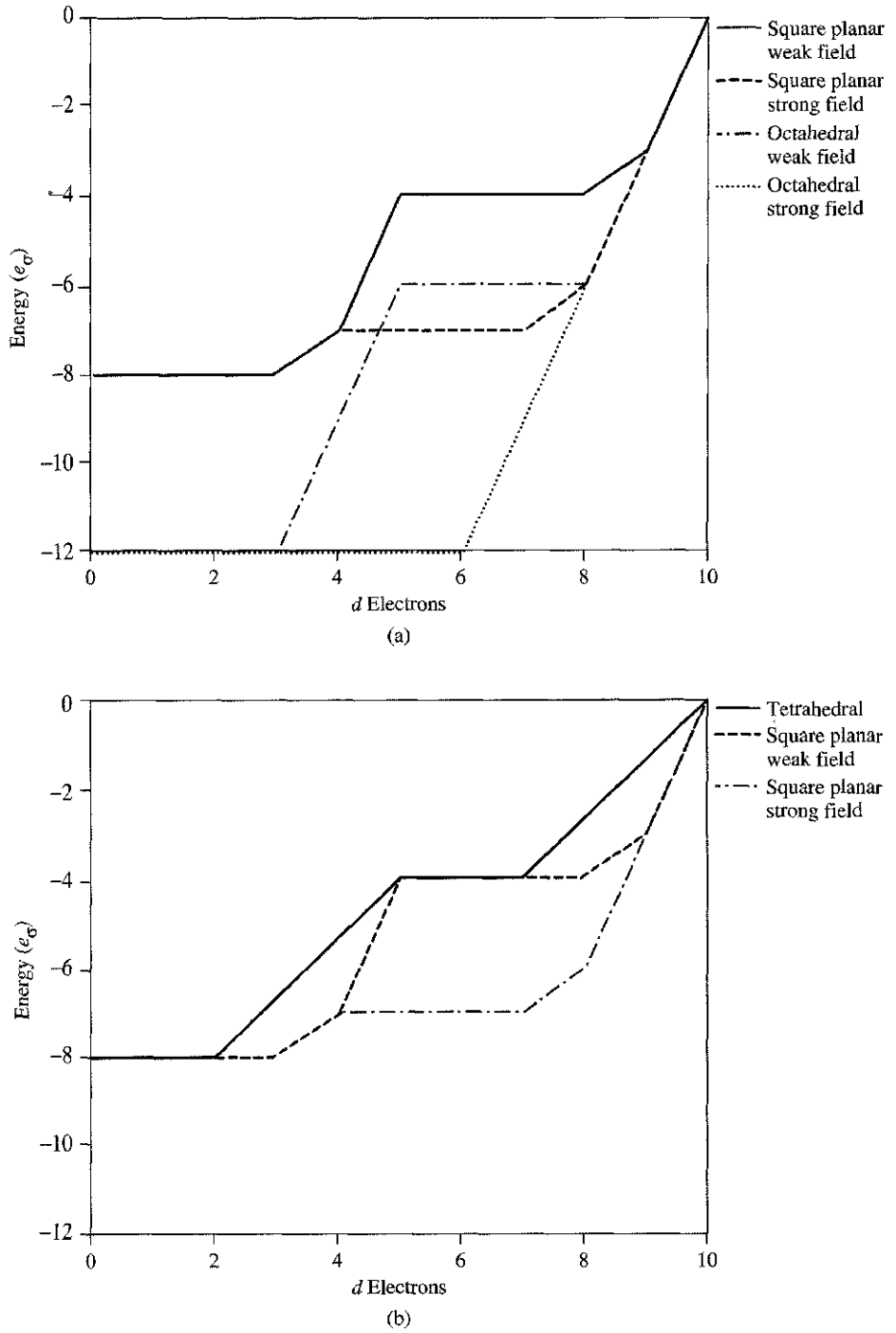

FIGURE 10-27 Angular Overlap Energies of four- and six-Coordinate Complexes. Only σ bonding is considered. (a) Octahedral and square-planar geometries, both strong- and weak-field cases. (b) Tetrahedral and square-planar geometries, both strong- and weak-field cases (there are no known low-spin tetrahedral complexes).

structures most commonly seen are tetragonal (four ligands in a square-planar geometry with two axial ligands at greater distances) and tetrahedral, sometimes flattened to approximately square planar. There are also trigonal-bipyramidal $[CuCl_5]^{3-}$ ions in $[Co(NH_3)_6][CuCl_5]$. By careful selection of ligands, many of the transition metal ions can form compounds with geometries other than octahedral. For d^8 ions, some of the simpler possibilities are the square-planar Au(III), Pt(II), and Pd(II) complexes. Ni(II) forms tetrahedral $[NiCl_4]^{2-}$, octahedral $[Ni(en)_3]^{2+}$, and square-planar $[Ni(CN)_4]^{2-}$ complexes, as well as other special cases such as the square-pyramidal $[Ni(CN)_5]^{3-}$.

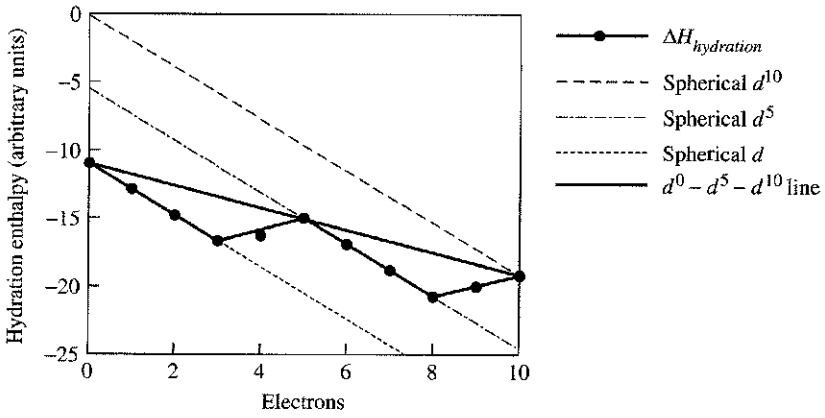

FIGURE 10-28 Simulated Hydration Enthalpies of M^{2+} Transition Metal Ions.

The d^7 Co(II) ion forms tetrahedral blue and octahedral pink complexes ($[CoCl_4]^{2-}$ and $[Co(H_2O)_6]^{2+}$ are simple examples), along with square-planar complexes when the ligands have strong planar tendencies ([Co(salen)], where salen = bis(salicylaldehyde-ethylenediimine) and a few trigonal-bipyramidal structures ($[Co(CN)_5]^{3-}$). Many other examples can be found; descriptive works such as that by Greenwood and Earnshaw[26] should be consulted for these.

10-7 OTHER SHAPES

Group theory and angular overlap can also be used to determine which d orbitals interact with ligand σ orbitals and to obtain a rough idea of the energies of the resulting molecular orbitals for geometries other than octahedral and square planar. As usual, the reducible representation for the ligand σ orbitals is determined and reduced to its irreducible representations. The character table is then used to determine which of the d orbitals match the representations. A qualitative estimate of the energies can usually be determined by examination of the shapes of the orbitals and their apparent overlap and confirmed by using the angular overlap tables.

As an example, we will consider a trigonal-bipyramidal complex ML_5, in which L is a σ donor only. The point group is D_{3h}, and the reducible and irreducible representations are shown here:

D_{3h}	E	$2C_3$	$3C_2$	σ_h	$2S_3$	$3\sigma_v$	*Orbitals*
Γ	5	2	1	3	0	3	
A_1'	1	1	1	1	1	1	s
A_1'	1	1	1	1	1	1	d_{z^2}
A_2''	1	1	−1	−1	−1	1	p_z
E'	2	−1	0	2	−1	0	$(p_x, p_y), (d_{x^2-y^2}, d_{xy})$

The d_{z^2} orbital has two ligand orbitals overlapping with it and forms the highest energy molecular orbital. The $d_{x^2-y^2}$ and d_{xy} are in the plane of the three equatorial ligands, but overlap is small because of the angles. They form molecular orbitals relatively high in energy, but not as high as the d_{z^2}. The remaining two orbitals, d_{xz} and d_{yz}, do not have symmetry matching that of the the ligand orbitals. These observations are enough to allow us to draw the diagram in Figure 10-29. The angular overlap method is consistent with these more qualitative results, with strong σ interaction with d_{z^2}, somewhat weaker interaction with $d_{x^2-y^2}$ and d_{xy}, and no interaction with the d_{xz} and d_{yz} orbitals.

[26]N. N. Greenwood and A. Earnshaw, *Chemistry of the Elements*, 2nd ed., Butterworth-Heinemann, Oxford, 1997.

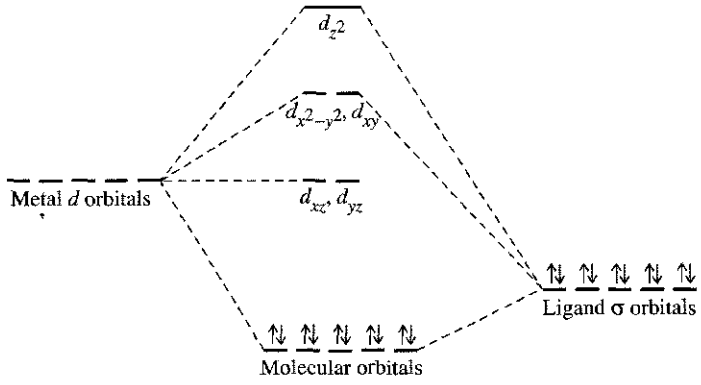

FIGURE 10-29 Trigonal-Bipyramidal Energy Levels. Metal *s* and *p* orbitals also contribute to the bonding molecular orbitals.

GENERAL REFERENCES

One of the best sources is G. Wilkinson, R. D. Gillard, and J. A. McCleverty, eds., *Comprehensive Coordination Chemistry*, Pergamon Press, Elmsford, NY, 1987; Vol. 1, *Theory and Background*, and Vol. 2, *Ligands*, are particularly useful. Others include the books cited in Chapter 4, which include chapters on coordination compounds. Some older, but still useful, sources are C. J. Ballhausen, *Introduction to Ligand Field Theory*, McGraw-Hill, New York, 1962; T. M. Dunn, D. S. McClure, and R. G. Pearson, *Crystal Field Theory*, Harper & Row, New York, 1965; and C. J. Ballhausen and H. B. Gray, *Molecular Orbital Theory*, W. A. Benjamin, New York, 1965. More recent volumes include T. A. Albright, J. K. Burdett, and M. Y. Whangbo, *Orbital Interactions in Chemistry*, Wiley-Interscience, New York, 1985; and the related text by T. A. Albright and J. K. Burdett, *Problems in Molecular Orbital Theory*, Oxford University Press, Oxford, 1992, which offers examples of many problems and their solutions.

PROBLEMS

10-1 Predict the number of unpaired electrons for each of the following:

a. A tetrahedral d^6 ion

b. $[Co(H_2O)_6]^{2+}$

c. $[Cr(H_2O)_6]^{3+}$

d. A square-planar d^7 ion

e. A coordination compound with a magnetic moment of 5.1 Bohr magnetons

10-2 Determine which of the following is paramagnetic, explain your choice, and estimate its magnetic moment.

$[Fe(CN)_6]^{4-}$ $[Co(H_2O)_6]^{3+}$ $[CoF_6]^{3-}$ $[RhF_6]^{3-}$

10-3 A compound with the empirical formula $Fe(H_2O)_4(CN)_2$ has a magnetic moment corresponding to $2\frac{2}{3}$ unpaired electrons per iron. How is this possible? (Hint: Two octahedral Fe(II) species are involved, each containing a single type of ligand.)

10-4 Show graphically how you would expect ΔH for the reaction

$$[M(H_2O)_6]^{2+} + 6\,NH_3 \longrightarrow [M(NH_3)_6]^{2+} + 6\,H_2O$$

to vary for the first transition series (M = Sc through Zn).

10-5 The stepwise stability constants in aqueous solution at 25°C for the formation of the ions $[M(en)(H_2O)_4]^{2+}$, $[M(en)_2(H_2O)_2]^{2+}$, and $[M(en)_3]^{2+}$ for copper and nickel are given in the table. Why is there such a difference in the third values? (Hint: Consider the special nature of d^9 complexes.)

	$[M(en)(H_2O)_4]^{2+}$	$[M(en)_2(H_2O)_2]^{2+}$	$[M(en)_3]^{2+}$
Cu	3×10^{10}	1×10^9	0.1 (estimated)
Ni	2×10^7	1×10^6	1×10^4